Biosensors and Bioelectronics 224 (2023) 115057

Contents lists available at ScienceDirect

Biosensors and Bioelectronics

journal homepage: www.elsevier.com/locate/bios

Integrated technologies for continuous monitoring of organs-on-chips: Current challenges and potential solutions

Jonathan Sabaté del Río [a], Jooyoung Ro [a,b], Heejeong Yoon [b], Tae-Eun Park [b,**], Yoon-Kyoung Cho [a,b,*]

[a] Center for Soft and Living Matter, Institute for Basic Science (IBS), Ulsan, 44919, Republic of Korea
[b] Department of Biomedical Engineering, Ulsan National Institute of Science and Technology (UNIST), Ulsan, 44919, Republic of Korea

ARTICLE INFO

Keywords:
Biosensors
Organ-on-a-chip
Microphysiological systems
Tissue chips
In vitro models

ABSTRACT

Organs-on-chips (OoCs) are biomimetic *in vitro* systems based on microfluidic cell cultures that recapitulate the *in vivo* physicochemical microenvironments and the physiologies and key functional units of specific human organs. These systems are versatile and can be customized to investigate organ-specific physiology, pathology, or pharmacology. They are more physiologically relevant than traditional two-dimensional cultures, can potentially replace the animal models or reduce the use of these models, and represent a unique opportunity for the development of personalized medicine when combined with human induced pluripotent stem cells. Continuous monitoring of important quality parameters of OoCs via a label-free, non-destructive, reliable, high-throughput, and multiplex method is critical for assessing the conditions of these systems and generating relevant analytical data; moreover, elaboration of quality predictive models is required for clinical trials of OoCs. Presently, these analytical data are obtained by manual or automatic sampling and analyzed using single-point, off-chip traditional methods. In this review, we describe recent efforts to integrate biosensing technologies into OoCs for monitoring the physiologies, functions, and physicochemical microenvironments of OoCs. Furthermore, we present potential alternative solutions to current challenges and future directions for the application of artificial intelligence in the development of OoCs and cyber-physical systems. These "smart" OoCs can learn and make autonomous decisions for process optimization, self-regulation, and data analysis.

1. Introduction

Organs-on-chips (OoCs) are emerging technologies that have the potential to emulate the functions, structures, and complex physiologies of *in vivo* tissues more accurately than traditional cell-based model systems. When combined with microsystems, microfluidics, and biomaterial technologies, OoCs facilitate precise control over cell culture conditions to sustain the resemblance of the key biochemical and physical features of the *in vivo* environment (Esch et al., 2015; Ingber, 2022). Particularly, the presence of compartments within the OoC allows the spatial arrangements of organ-specific cell types to imitate the fundamental morphology of the organ and the manipulation of intercellular communication. For example, tissue barriers composed of an epithelial monolayer separated by tissue-specific endothelium can be recapitulated by placing each cell type in different compartments (Huh et al., 2010). In addition, a 3D vessel-like structure is reconstituted in an ECM hydrogel-filled microchannel by placing the mesenchymal cells releasing angiogenic factors in a separate channel (Kim et al., 2013), or by culturing the endothelial cells in tubular-shaped hollow channel (Herland et al., 2016). The use of microfluidic systems in OoCs permits an optimal supply of nutrients and oxygen to these cell types and removes metabolic waste from them by delivering different cell culture media via compartmentalized microchannels. Moreover, OoCs often comprise physicochemical stimuli, such as electrical pulses, to enable organ-specific functionality and cell maturation. These systems facilitate simulation, mechanistic investigation, and pharmacological modulation of complex biological processes (Ingber, 2022).

OoC is not only a powerful platform for physiological studies, but also an interesting test platform for drug discovery and delivery and personalized medicine (Fig. 1A). According to several studies, preclinical animal models are inadequate predictors of human toxicities and drug responses (Wong et al., 2019), resulting in high failure rates of new

* Corresponding author. Center for Soft and Living Matter, Institute for Basic Science (IBS), Ulsan, 44919, Republic of Korea.
** Corresponding author.
E-mail addresses: tepark@unist.ac.kr (T.-E. Park), ykcho@unist.ac.kr (Y.-K. Cho).

https://doi.org/10.1016/j.bios.2022.115057
Received 30 June 2022; Received in revised form 29 December 2022; Accepted 30 December 2022
Available online 2 January 2023

drugs in clinical trials. As increasing evidence suggests that the use of OoCs instead of animal models leads to more clinically relevant outcomes, human OoCs may potentially replace animal models or reduce the use of these models. Furthermore, OoCs offer a more controllable assay environment at a lower cost with higher manufacturing throughput and the ability to integrate real-time monitoring biosensors. Personalized OoCs based on human induced pluripotent stem cells (iPSCs) can be employed for precision medicine functional analysis, which considers genetic differences between individuals.

Since the discovery of the first OoC that simulates human pulmonary alveoli (Huh et al., 2010), many other OoCs have been developed including liver-on-a-chip (Rennert et al., 2015), heart-on-a-chip (Kujala et al., 2016), intestine-on-a-chip (Kim and Ingber, 2013), kidney-on-a-chip (Jang et al., 2013), blood–brain barrier (BBB)-on-a-chip (Park et al., 2019), eye-on-a-chip (Chung et al., 2018), and bone marrow-on-a-chip (Chou et al., 2020). This field has progressed to the point where different OoCs can be integrated together to recapitulate higher-order interactions between organs, resulting in the development of multi-organ systems known as "human body-on-chips" (Low et al., 2021; Novak et al., 2020). Nevertheless, formal validation of the replacement of animal models with OoCs will possibly take time and requires the active participation of other researchers in the pharmaceutical industry and government agencies that regulate drugs. This should include testing commonly agreed reference compounds and comparing with clinical data to value the output from OoCs. Comparative transcriptomic and proteomic analysis between OoCs and human tissues will provide insight into similarities between OoCs and target organs. In addition, technical advancements for higher-throughput systems are required to use the OoCs at the early stage of drug discovery, considering that many current OoCs have been developed to test a small number of selected lead compounds. Even though there are many technical hurdles to overcome before replacing the animal models, many researchers agree with the potential of OoCs and a variety of efforts have been undertaken to promote OoCs as standardized platforms in a drug discovery pipeline.

Monitoring cell behaviors is just as important as recapitulating the biological responses of *in vivo* tissues. Integration of *in situ* monitoring devices capable of continuously observing cell behaviors in real time with OoCs can provide information about crucial biological parameters that should be addressed during every cultivation. Measurement of metabolites and secreted proteins, for example, cytokines, is also necessary for understanding the cell biology in response to drugs, external stimuli, cell–cell communication, and pathological conditions. Extracting this complex information from OoCs in a high-throughput and multiplexed manner is critical for the successful adoption of this technology in broad industries and eventually in translational medicine (Low et al., 2021).

Currently, the relevant analytical information from OoCs is acquired via off-chip assays, such as microfluorimetry, enzyme-linked immunosorbent assay (ELISA), qPCR, sequencing, and mass spectroscopy, because of the technical challenges in establishing on-chip analysis systems (Kavand et al., 2022). However, off-chip measurements are generally time-consuming, labor-intensive and require large volumes. More importantly, downstream end-point analysis do not consider the spatial or temporal resolutions of organ-specific cell types needed to examine dynamic phenomena and local gradients. Nevertheless, continuous and long-term monitoring of bioanalytes in complex media using the existing biosensing systems is hindered by several technical challenges including biofouling passivation, lack of robustness, scarcity of real-time and continuous monitoring schemes, and surface saturation (Fuchs et al., 2021).

In this review, we focus on the current state-of-the-art and technical challenges in integrated on-chip biosensing monitoring technologies and the potential solutions that can be explored to achieve significant milestones in the biosensing field. Additionally, we discuss the combination of artificial intelligence and sensor-integrated OoCs as a promising prospect in translational medicine.

2. Cyber-physical systems

Microfluidics allow the development of systems for manipulation of fluids with reproducibility and precision to generate analytical information (Chiu et al., 2017). Machine intelligence provides predictive tools with the ability to learn from data by leveraging multimodal monitoring and data-acquisition instrumentation. The convergence of microfluidic platforms and artificial intelligence has potential for operating such systems autonomously via closed-loop data-driven models. In this context, machine learning algorithms can be powerful

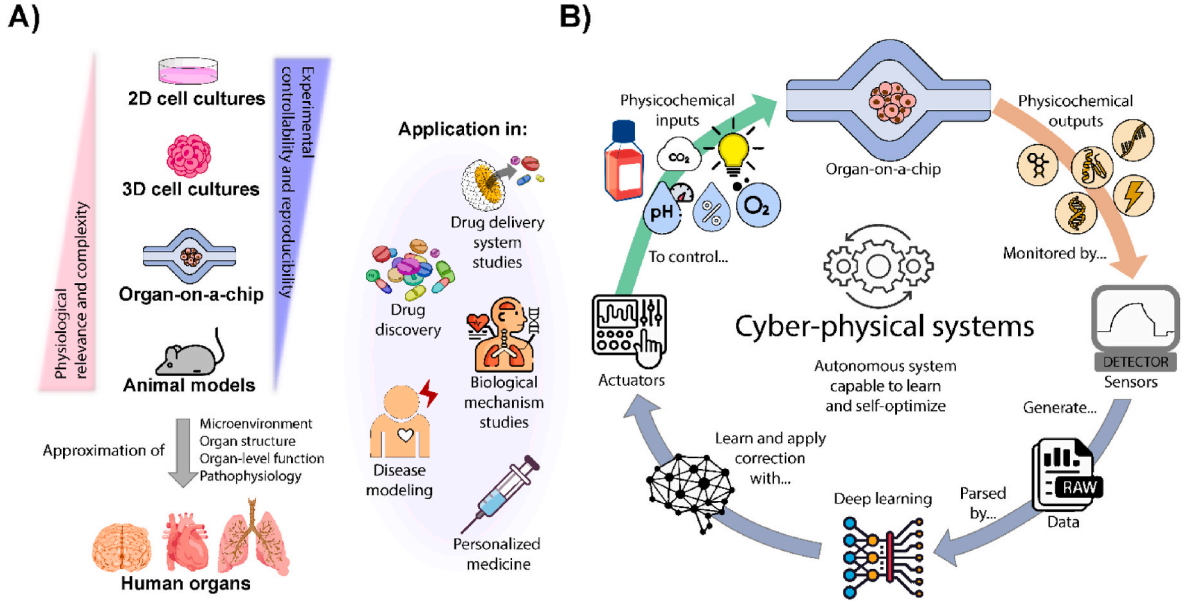

Fig. 1. A) Schematic of biological systems used to mimic human microphysiological systems and their applications. **B)** Concept of cyber-physical system integrated with on-chip sensors to monitor physicochemical cues (outputs) from OoCs. The obtained data can be analyzed by deep learning algorithms to learn and apply a correction of physicochemical stimuli (inputs) using actuators.

tools for closing the loop of information feedback obtained from OoCs, and generating numerous meaningful outputs (Isozaki et al., 2020). Large datasets obtained from integrated monitoring devices can be used to extract relevant information about cell physiology from OoCs (Young et al., 2019) (Fig. 1B). Moreover, these algorithms can enable autonomous decision-making and retroactive changes in input parameters to offer optimal physicochemical stimuli depending on the cell conditions and microenvironments in the OoC (Fig. 1B).

OoCs have the potential to become high-throughput platforms for drug screening and drug safety evaluation (Esch et al., 2015), considering the general definition of high-throughput as a process that is scaled up to conduct many tests, usually via increased levels of automation. However, the fabrication of OoCs is based on laborious and not standardized methodologies that require constant human intervention. Although this is suitable for fabrication of the small number of OoC required for academic studies, true validation of their use as animal replacements will require standardized and automated manufacturing using reproducible and reliable processes to achieve the large-scale evaluation required for clinical assays (Ingber, 2022). The use of microfluidic platforms with the integration of artificial intelligence for the production, control, and analysis of processes addresses this need of automation for achieving high-throughput analysis platforms. OoCs with self-regulatory systems would achieve a precise control of the physicochemical microenvironment during normal organogenesis, maintain homeostasis of OoCs or sustain the life cycles of OoCs for extended periods of time, so that the OoC can be ready to be used on demand (Galan et al., 2020; Young et al., 2019).

The convergence of machine intelligence and microfluidics represents an emerging field with applications in diagnostics (Liu et al., 2021), disease treatment (Zare Harofte et al., 2022), material synthesis, and drug discovery (Schneider, 2018). Although the integration of real-time and continuous monitoring for artificial biological systems has not been achieved yet, the vision of self-regulated OoC has already been proposed by other researchers as well (Galan et al., 2020; Wikswo et al., 2013; Young et al., 2019).

3. Integration of monitoring systems with OoCs

OoCs must recapitulate the main functional elements of the organ that is modelled. Maintaining and controlling a representative physical microenvironment of the *in vivo* organ, while extracting meaningful information, is crucial to achieve reliable, robust, and reproducible *in vitro* models. Therefore, the physicochemical parameters can be classified into two categories: input parameters that need to be controlled and output parameters that should be monitored. Dissolved oxygen, temperature, light exposure, medium composition, flow shear stress, vibration, and other external stimuli are examples of input parameters (Fig. 2A). Although miniaturized and easily integrated actuators are commercially available for controlling the input parameters of OoCs, the biosensing technologies required to continuously read the output parameters in real time are lacking (Fig. 2B). Integration of biosensors with OoCs to acquire analytical information *in situ* is critical for understanding the physiological functionalities, which include cell morphology, cell viability, secretion of specific biomarkers, and other physicochemical cues, of cultured cells within OoCs and their responses to external stimuli (Fig. 2C).

4. Types of OoC-monitoring techniques

4.1. Off-line monitoring techniques and assays

Although the focus of this review is on integrated on-chip biosensing techniques, approaches based on on-line and off-line strategies need to be briefly mentioned (Fig. 2B). By on-chip we refer to technology directly embedded in the OoC, whereas by on-line we define technology integrated in a different microfluidic device connected to the OoC with tubbing (Lin et al., 2020). On-line approaches utilize miniaturized lab-on-a-chip microfluidic solutions and are plug-and-play approaches that provide versatility to the setup, impose fewer design restrictions, allow quick replacement, and offer fewer constraints to biosensing strategies because all the assay steps are conducted off-chip in a different lab-on-chip module (Lin et al., 2020). Lab-on-a-chip, also known as a micro total analysis system, is an autonomous microfluidic chip that integrates all the steps, such as sample preparation, mixing, reaction, separation, cell culture, sorting, lysis, and detection, required to perform a full assay (Shi et al., 2019).

Off-line detection methods are based on sampling from the OoC, either manually or in an automated fashion, to be analyzed on-site or off-site by traditional analytical tools, for example, mass spectrometry, ELISA, staining techniques, electrophoresis, polymerase chain reaction, flow cytometry, and microfluorimetry (Esch et al., 2015; Li and Tian, 2018).

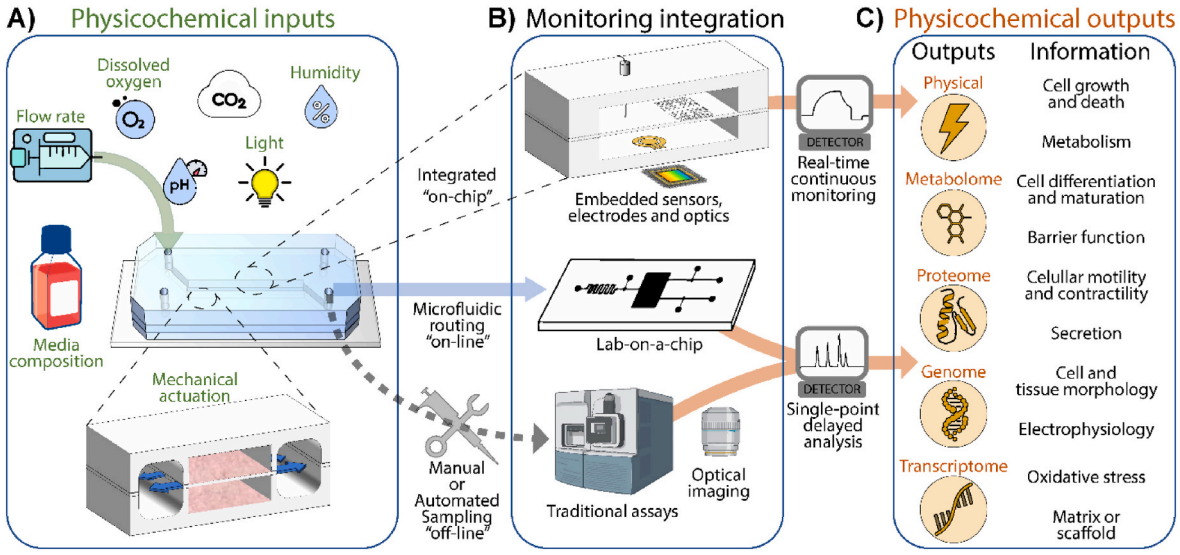

Fig. 2. A) Examples of different physicochemical inputs. **B)** Classification of monitoring strategies based on the degree of integration and detection modality. **C)** Physicochemical outputs that can be extracted from various assays and examples of the analytical information with which the physicochemical outputs can be correlated.

4.2. On-chip monitoring techniques

On-chip integration of sensing technologies in OoC has not been accomplished yet for most relevant physicochemical cues. There are technical challenges associated with material biocompatibility or optical transparency, sensor lifetime and long-term biofouling, sensor robustness in cell medium, lack of miniaturization, surface saturation, need for calibration, lack of sufficient sensitivity and detection limit, response time, etc. Moreover, for some cases the use of on-chip sensing may not be necessary if the available off-chip strategies provide a sufficient sampling or sensing rate to match the speed of the biological process being monitored.

The effort of developing and embedding on-chip sensing technologies is justified in cases when real-time and/or continuous monitoring is required and available off-chip technologies are insufficient to provide the detection limit, sensitivity or spaciotemporal resolution required. In-line microfluidic modules and off-line strategies introduce a delay in the measurement, whereas off-line analysis only provides discrete end-point measurements. Integration of real-time and continuous data acquisition in OoCs combined with artificial intelligence presents a fertile ground for the development of "smart" OoCs. In the future, these platforms may also be useful for screening the influence of unknown physicochemical factors or unknown fast dynamics in certain pathophysiological processes. In order situations, the short lifespan of some biomarkers (e.g., some reactive oxygen species) may limit the diffusion time required to reach the sensor and placement of the sensing elements near the source is necessary.

Moreover, the small number of biomarkers secreted by the relatively small set of cells used in OoC, as well as the added dilution effect of sampling or flowing out into off-chip microfluidic modules, may yield concentrations below the detection limit and sensitivity specifications of available sensing technologies. Also in this cases, integration of sensors in close proximity to the source may prevent analyte dilution and yield higher sensing signal outputs.

Additionally, the analysis of some physicochemical cues needs to be conducted *in situ* or may require two-/three-dimensional (2D/3D) spatial resolution. Many examples cited in this review fit this case, including transepithelial/endothelial electrical resistance measurements for membrane permeability; electrochemical impedance measurements for tracking the spheroid size or cell viability; optical imaging to assess cell morphology, motility, or cell tracking; extracellular field potential measurements for electrophysiological studies; and piezoelectric and optical measurements of mechanical cell strain/contraction in muscle and skeletal cells. Other potential examples include the monitoring of oxygen gradient in a spheroid with a necrotic core during organogenesis, evaluation of the secretome and role of different cells in a co-culture, or visualization the gradient and influence of chemical factors to better understand specific cell-to-cell interactions.

Finally, the specific sensor quality parameter requirements in integrated technologies will depend strongly on the OoC model used, the analyte that needs to be monitored, the study performed and the sensing technology used for such a task. Therefore, it is impossible to define a priori what would be the best sensing technology to use, what materials will be more suitable, or to define other quality parameters like the sensitivity, detection limit, response time or sensor lifespan. The conceptualization and design of the OoC will be ultimately defined by the purpose of the experiments, the organ model used, the experimental conditions, the physicochemical cues being monitored and the available sensing technologies.

The reader may benefit from other reviews that analyze in depth the current state of the art regarding sensor integration in OoCs (Kilic et al., 2018), provide general guidance on the rationale design and technological aspects related to integration of sensing technologies (Young et al., 2019) regarding fabrication methods or selection of biological elements (Fuchs et al., 2021), selection of chip or sensor and microfluidic materials (Leung et al., 2022).

4.2.1. Sensors

Sensors are analytical devices that produces an output signal for the purpose of sensing a physicochemical phenomenon and are divided into physical and biochemical sensors. Biochemical sensors are composed of three parts: a receptor or sensing element, signal transducer, and detector. The receptor selectively interacts with the target analyte and is either a synthetic or biological element with binding affinity to the analyte or catalytic activity toward it. This interaction is converted into an electric signal that can be measured and quantified by the detector via the transducer.

Common catalytic receptors include enzymes (Nguyen et al., 2019), metal–organic frameworks (Anik et al., 2019), nanoparticles (Białas et al., 2022), and nucleic acids (Yang et al., 2021). In contrast, affinity-based binding receptors comprise ion-selective membranes (Hu et al., 2016), molecularly imprinted polymers (Pohanka, 2017), deoxyribonucleic acid (DNA) (Rafique et al., 2019), aptamers (Zhao et al., 2022), antibodies (Kokkinos et al., 2016), peptides (Karimzadeh et al., 2018), phages (Paramasivam et al., 2022), whole cells (Eltzov and Marks, 2011), and non-immunoglobulin scaffolds (Škrlec et al., 2015).

Unlike the cases of catalytic biosensors, a problem inherent to affinity-based biosensors is that the binding between the receptor and the analyte is often irreversible due to the high affinity constant, resulting in surface saturation (Goode et al., 2015). Therefore, continuous monitoring is not feasible. This is not an issue for diagnostic applications, which typically require end-point detection; however, this problem renders continuous monitoring inconvenient because the surface must be regenerated prior to each use. Although surface regeneration has been conducted for on-line biosensors (Zhang et al., 2017), it cannot be performed without killing, damaging, or affecting the cells when the sensors are placed *in situ*, that is, inside the OoC.

Depending on their transduction mechanisms, sensors can be classified into the following groups: mechanical (Chalklen et al., 2020), optical (Chen and Wang, 2020), and electrical and electrochemical (bio) sensors (Singh et al., 2021). In subsequent sections, details of the various sensing principles for each type of sensors are provided.

4.2.1.1. Electrochemical sensors. The primary working principle of an electrochemical sensor is based on the transduction of a selective (bio) chemical interaction into an electric signal. According to the physical properties being measured, the electrochemical sensors can be divided into three different categories: potentiometric, voltammetric, and impedimetric sensors. Electrochemical sensors are highly attractive for integration with OoCs because of their inherent simplicities, easy miniaturizations, low costs, and excellent analytical performances. Numerous studies have been reported on the integration of electrochemical biosensors with microfluidic devices (Schmidt-Speicher and Länge, 2021) and the biological and biomedical applications of the resulting integrated systems (Maduraiveeran et al., 2018).

Typically, potentiometric sensors are employed for the analysis of ions, for instance, sodium and potassium ions, pH, and carbon dioxide. The working principle of an impedimetric sensor is based on the application of a voltage in the direct current mode and measurement of the resulting resistance for resistive/conductometric or capacitive sensors or the introduction of an alternating current at several frequencies and evaluation of the impedance spectrum. Voltammetric sensors, such as the glucometer, have been widely used in diagnostics, and their working principle relies on the measurement of the current output upon application of an electric potential. This electric potential drives a charge-transfer reaction of the receptor with the analyte (for example, reduction of oxygen) or with a byproduct of a catalytic reaction (oxidation of peroxide, a byproduct of the enzymatic catalysis of glucose). This strategy has been successfully applied to monitor metabolic analytes, such as glucose (Hassan et al., 2021; Hwang et al., 2018), lactate (Shakhih et al., 2021), uric acid (Hernández-Ramírez et al., 2021), oxygen (Suzuki et al., 2001), and hydrogen peroxide (Shamkhalichenar

and Choi, 2020), in OoCs. As the readout reaction is irreversible, it disturbs the OoC microenvironment; nevertheless, the measurements can be continuously conducted.

Many analytes lack catalytic activities or are not associated with enzymes that catalyze them. In this case, the detection strategy is usually based on affinity-based interactions of analytes with enzymatic labels (for instance, horseradish peroxidase-labeled antibodies). However, to detect an analyte by a sensor, a reagent, an enzymatic substrate, and/or a label must be used. Although this is an acceptable approach for end-point assays, its implementation in real-time continuous monitoring of analytes can be difficult. In contrast, both potentiometric and impedimetric sensors can operate in label- and reagent-free modes.

4.2.1.2. Electrical sensors. Temperature can be measured via the associated change in the resistance of a conductor within a linear range. The same principle can be used to evaluate flow speed of a liquid. If a conductor heated via the Joule effect is exposed to a flowing liquid, it will experience thermal loss proportional to the flow speed of the liquid. This phenomenon can be utilized to calculate the shear stress experienced by the cells in a microfluidic channel (Booth et al., 2014). For OoCs, including lung-on-a-chip, with airway microchannels, humidity is an important parameter to consider. Because these systems also undergo strain and expansion as a part of their stimuli microenvironment, flexible humidity sensors are needed and have been reported (Anum Satti et al., 2018; Barmpakos and Kaltsas, 2021). Although to date, the application of these sensors in OoCs has not been reported, impedance measurements on an interdigitated microelectrode have been used to report miniaturized and integrable flexible options compatible with long epithelial cells (Soomro et al., 2019).

4.2.1.3. Mechanical, electromechanical, and mechano-optical sensors. Mechanical sensors can measure mechanical deformations and forces and convert them into optical or electrical signals (Chalklen et al., 2020). A simple approach is to use micropillars to calculate the forces from cells according to the degrees of mechanical deformations in the micropillars (Tan et al., 2018). A piezoelectric transducer can detect small movements or forces and consequently generate electric currents. Piezoelectric microcantilevers can also work in dynamic modes, vibrating at a resonant frequency upon the application of electrical stimulation. A phase shift in the resonant frequency or an optical shift can produce a signal, as in the case of atomic force microscopy.

Surface acoustic wave (SAW) sensors are based on the actuation of an interdigitated pair of electrodes on a piezoelectric surface by a high-frequency voltage. Electromechanical coupling emits a traveling acoustic wave into the media, and the frequency proportionally shifts in the presence of the target analyte. Quartz crystal microbalance is a type of SAW sensor that utilizes a piezoelectric crystal for sensing (Go et al., 2017). The frequency of the oscillating crystal is sensitive to the contact medium, and the shift in the resonance frequency is proportional to the change in mass coupled to the surface of the crystal. This strategy can be used to monitor variations in the density of the medium and has been successfully employed to examine cell adhesion, morphology, mechanics, motility, and signaling (Chen et al., 2018).

These sensing modalities offer non-invasive, label-free, and real-time monitoring of both mass and mechanical properties. The above-mentioned sensors have been miniaturized and integrated with microfluidics for chemical and biochemical analysis (Go et al., 2017).

4.2.1.4. Optical sensors. Optical sensors are a wide range of devices that measure the properties, such as intensity, refractive index, and scattering, of electromagnetic radiation. Optical sensors have been extensively integrated with microfluidic chips (Liao et al., 2019) owing the intrinsic transparency of the materials typically used for the fabrication of OoC. However, not all OoCs are transparent or suitable to be monitored with optical sensors. Although optical waveguides and other optoelectronic components have been miniaturized and integrated into microfluidic devices, optical instrumentation is generally more expensive and complex and its miniaturization and integration into OoCs is more challenging than those of electrochemical setups (Pires et al., 2014). However, via optical sensors, real-time continuous monitoring of analytes can be achieved without the need for physical contact between the instrument and the sensing surface. These are attractive advantages because they provide a minimally invasive multiplexed means for long-term OoC monitoring, for as long as the use of dyes or labeling steps are not required. Owing to these advantages, numerous optical sensors have been developed using several detection methods including refractometry (Li et al., 2017), absorbance (Martín-Palma, 2021), luminescence (Roda et al., 2016), and surface-enhanced Raman scattering (SERS) (Serebrennikova et al., 2021).

Absorbance detection relies on the measurement of light attenuation produced by a specific analyte. For example, non-dispersive infrared sensors have been employed to detect carbon dioxide (Tipparaju et al., 2021). If an analyte does not absorb light, a dye that reacts with the analyte can be used (Mousavi Shaegh et al., 2016). Alternatively, a label that interacts with the analyte or a by-product of a specific reaction can be utilized. Although this detection scheme is simple and easily integrable, its application is hampered by the fact that the attenuation is proportional to the optical path of the substrate, and thus, the sensitivity proportionally decreases in small reaction chambers, typical those of microfluidic devices. Similarly, in the case of luminescence detection, a dye is excited by light, and after a certain lifetime, the molecule relaxes by emitting a photon. Although there are specific dyes for monitoring oxygen, pH, and various ions, this technique is often temperature-sensitive.

Surface plasmon resonance (SPR) (Liu and Zhang, 2021) is one of the most extensively used plasmon-based refractometric techniques. Plasmons are collective oscillations of free electrons generated by the interaction of incident light with a metal nanostructure at a metal–dielectric interface. These plasmons produce an evanescent field that penetrates the surrounding media and is sensitive to the changes in the refractive index of the incident light at the metal–dielectric interface caused by biochemical reactions. SPR has been used in numerous applications, for example, prism coupling, waveguides, and gratings. Moreover, substrate configuration plays a significant role in enhancing the formation of plasmons, and various periodic nanostructures, such as nanohole and nanoparticle arrays, have been used for SPR. A key advantage of SPR over other optical methods is that it can operate without dyes and labels and thus should be considered if continuous monitoring of OoCs is required.

SERS (Langer et al., 2020) is another technique that utilizes the plasmonic coupling effect for enhancing the vibrational signals in Raman spectra. SERS spectra can offer a high degree of chemical structure information, and therefore, SERS can be used for the direct fingerprinting of compounds. The spectrum of each compound can potentially be compared with those of known compounds for identification.

4.2.2. Electrical measurements

Electrical measurements have been widely adopted and integrated into OoCs for evaluating transepithelial/endothelial electrical resistance (TEER), electric cell-surface impedance, and extracellular field potentials. To measure the TEER value in an OoC device, two electrodes are placed on opposite sides of the barrier, but alternatively a set of four electrodes can be used to eliminate the contribution of contact and lead resistances (Elbrecht et al., 2016). The TEER is calculated by analyzing and fitting the impedance spectra obtained for the electrodes placed across a semipermeable tissue membrane (Miyazaki et al., 2021). TEER facilitates non-disruptive, continuous, and real-time monitoring of the integrities and permeabilities of tissue barriers. Physiological resemblance of an OoC can be assessed by comparing the TEER acquired *in vitro* with the typical TEER obtained *in vivo*. Electric cell-surface

impedance sensing (ECIS) is based on the analysis of impedance at a specific frequency across a cell layer on the electrodes using a two- or three-electrode configuration (Zhang and Jang, 2018). ECIS can be employed to investigate cell attachment and junctions (Janshoff et al., 2010). Furthermore, as the impedance increases with a decrease in the available surface area of the electrode, ECIS can be used for the real-time monitoring of cell growth and morphology (Binder et al., 2021). Extracellular field potentials are generated from electrically active cells, including cardiomyocytes, insulin-producing islets, and neurons, and can be recorded using open-circuit potential electrodes placed in close contact with these cells (Spira and Hai, 2013). Because a high spatio-temporal resolution is required to acquire the activities of cells at different frequencies, these measurements are typically performed using dense ultramicroelectrode arrays on which the cells are seeded.

4.2.3. Optical measurements

The most common technique used for monitoring OoCs is the optical inspection of OoCs by an inverted microscope to control the state of the cell culture and experiment. Researchers usually regulate the sizes, numbers, and shapes of the cells and analyze failures such as chip delamination, air bubbles, and bacterial contamination. This method is subjective as an external observer is needed to assess the condition of a tissue section or the general states of cells. Different observers may arrive at different conclusions or fail to identify specific features depending on their own experiences. Moreover, this method is time-consuming for the researcher, provides only qualitative, single time-point analysis, and is impossible to automate. Nevertheless, optical imaging acquisition equipment can be miniaturized and integrated into OoCs for on-chip microscopy to enable high-throughput analysis of multiple chips and reduce the space and costs associated with the use of bulk instrumentation (Kim et al., 2012; Takehara et al., 2017; Zhang et al., 2015). Artificial intelligence is a powerful tool that offers an exciting new approach to the analysis and use of image-based data in OoCs. Deep learning, the most representative research field in artificial intelligence, is an emerging area of research in the field of machine learning for automation. Deep learning has been implemented in cell cultures grown ion microfluidic chips for cell classification, location, and tracking, target recognition, and image segmentation (Li et al., 2022).

Other optical measurements utilize spectroscopic analysis techniques, for instance, Raman scattering and SERS (Das and Agrawal, 2011). Direct analysis of the samples facilitates fast, convenient, and sensitive acquisition of molecular vibrational spectra of their chemical compositions. Subsequently, these spectra can be compared with a library of spectra of pure compounds to extract the "fingerprints" and determine the biochemical compositions of the samples.

5. Monitoring of physicochemical parameters

The most extensively used strategies for the monitoring of OoCs rely on optical sensors and imaging (Fig. 3A), electrical measurements (Fig. 3B), and electrochemical sensors (Fig. 3C). Optical and electrochemical sensors are typically used to detect the presence of biochemical signals via catalytic or enzymatic breakdown or affinity binding, whereas electrical measurements are employed to monitor cell membrane integrity. Mechanical sensors are also being explored in this regard due to their inherent label-free and continuous biosensing capabilities (Fig. 3D). In contrast, electrical sensors are widely used to

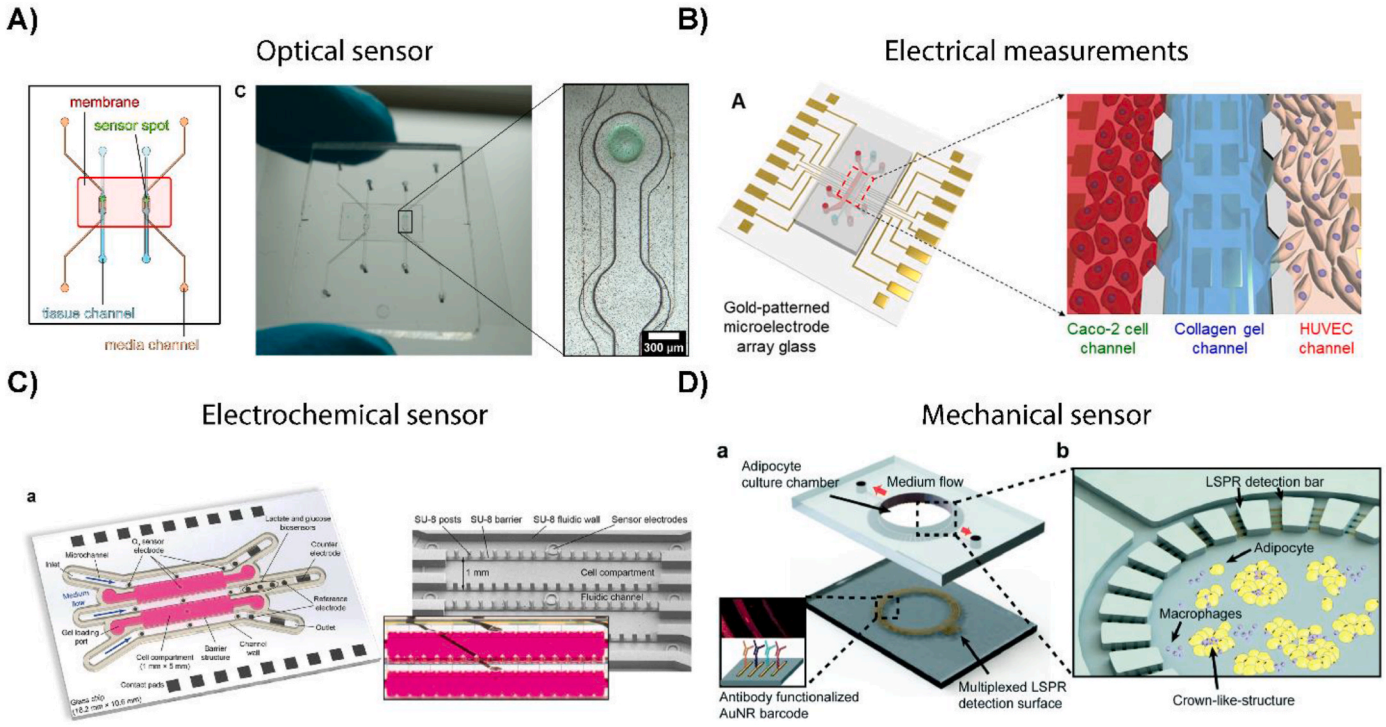

Fig. 3. Integration of various sensors into OoCs. **A)** Heart-on-a-chip embedded with oxygen optical sensors. Sensors were developed using optical fibers, and the results were read using a phase fluorimeter (Schneider et al., 2022). **B)** Adipose tissue-on-a-chip integrated with antibody-conjugated localized surface plasmon resonance (LSPR) barcode sensor arrays. Cytokine concentrations were measured via intensity changes by dark-field imaging and antibody-conjugated gold nanorod (AuNR) LSPR biosensors (Zhu et al., 2018). **C)** Gut-on-a-chip with gold-patterned microelectrode arrays. Epithelial barrier functions were evaluated by electrochemical impedance spectroscopy (Jeon et al., 2022). **D)** Breast cancer-on-a-chip integrated with an electrochemical microsensor for the detection of lactate, glucose, and oxygen. A poly(2-hydroxyethyl methacrylate) (pHEMA)-based hydrogel immobilized on the electrodes measures the equimolar conversion of glucose or lactate into H_2O_2 (Dornhof et al., 2022). Panel A is reproduced with permission from Schneider et al. (2022). Copyright 2022 Elsevier. Panel B is reproduced with permission from Zhu et al. (2018). Copyright 2018 Royal Society of Chemistry. Panel C is reproduced with permission from Jeon et al. (2022). Copyright 2022 Springer Nature. Panel D is reproduced with permission from Dornhof et al. (2022). Copyright 2022 Royal Society of Chemistry.

monitor physical parameters such as temperature, flow rate, and mechanical responses. Table 1 presents the various physicochemical parameters monitored in OoCs and the specific measurement or sensing techniques employed in each case.

5.1. Cell properties

5.1.1. Cellular barrier integrity

To verify the mimicry and functionality of various cellular barriers existing in the body, the barrier integrity is primarily observed. Typically, TEER (Table 1), which measures the electrical resistance formed by barriers, and the determination of apparent permeability using fluorophores (Apostolou et al., 2021; Arık et al., 2018; Park et al., 2019) are mainly used.

The importance of TEER measurement has been highlighted in BBB (Badiola-Mateos et al., 2021; Bossink et al., 2021; Falanga et al., 2017; van der Helm et al., 2016, 2017; Li et al., 2022; Park et al., 2019; Ugolini et al., 2018; Vatine et al., 2019), intestine (Bossink et al., 2021; Jeon et al., 2022), kidney (Choudhury et al., 2022; Shaughnessey et al., 2022) and lung (Henry et al., 2017; Khalid et al., 2020; Mermoud et al., 2018) models, where cell barrier integrity is a critical indicator of the (patho) physiological statuses of OoCs. OoCs incorporated with conductors, including silver/silver chloride (Ugolini et al., 2018; Wang et al., 2017), gold (Jeon et al., 2022; Park et al., 2019; Vatine et al., 2019), and platinum electrodes (Bossink et al., 2021; van der Helm et al., 2016, 2017), have enabled the measurement of the barrier integrity of these endothelial and epithelial models. The BBB, a unique and selective physiological barrier that regulates the transport of substances between the blood and the central nervous system (CNS), plays an important role in maintaining homeostasis for proper brain function. The BBB is formed by the brain microvascular endothelium, pericytes that encircle the endothelium, and astrocytes extending process that ensheath the blood vessel. The tight structure in which glial cells tightly surround the brain microvascular endothelial cells prevents drugs or metabolites from entering. Since BBB represents a major obstacle for CNS drug delivery, a predictive model for the BBB permeability of substances is strongly required (Lee and Leong, 2020; Park et al., 2019). Thus, numerous BBBs-on-chips have been constructed to serve as tools for the analysis of the BBB permeabilities of drugs. To avoid the production of false-positive results, these models must have strong barrier functions at the level of *in vivo* BBB.

The TEER measurement on BBB-on-a-chip can facilitate the optimization of BBB culture conditions (Park et al., 2019; Wang et al., 2017), monitoring of cell barrier function to determine the optimal day for using the BBB-on-a-chip (Badiola-Mateos et al., 2021; Bossink et al., 2021; Falanga et al., 2017), modeling of the disorders, such as monocarboxylate transporter 8 (MCT8) deficiency, affecting the BBB permeability (Vatine et al., 2019), and discovery of BBB regenerative medicines. The effects of brain endothelial differentiation conditions on the barrier formation of BBB-on-a-chip have been successfully investigated by comparing the daily TEER values of BBBs-on-chips established by new versus past maturation methods (Park et al., 2019). Additionally, the efficacy of the osmotic opening of BBB, which loosens the tight junctions of brain endothelial cells to enable the delivery of large-sized drugs, has been analyzed by measuring the TEER values in real time, indicating a decrease in barrier integrity in hypertonic media and a rapid recovery of barrier integrity in isotonic media under fluid flow (Park et al., 2019).

The gut epithelial layer also provides an important physiological barrier that separates the gut lumen from the lamina propria. It facilitates the transcellular movements of ions and nutrients and restricts paracellular transport of gut microbes, food antigens, and toxins (Assimakopoulos et al., 2018). However, the intestinal barrier is disrupted by many factors including enteric infection, antibiotics, circadian rhythm, and release of hormones owing to psychological stress (Assimakopoulos et al., 2018). Thus, TEER monitoring is crucial to

Table 1
Representative organs-on-chips (OoCs) integrated with on-chip sensors.

Biomarker/target signal	Model	Detection method	References
Membrane permeability	BBB	Electrical measurements: EIS	(Badiola-Mateos et al., 2021; Bossink et al., 2021; Falanga et al., 2017; van der Helm et al., 2017, 2016; Park et al., 2019; Vatine et al., 2019)
		Electrical measurements: EIS	(Ugolini et al., 2018; Wang et al., 2017)
	Gut	Electrical measurements: EIS	(Bossink et al., 2021; Jeon et al., 2022)
	Lung	Electrical measurements: EIS	(Henry et al., 2017; Mermoud et al., 2018)
	Lung cancer	Electrical measurements: EIS	(Khalid et al., 2020)
	Heart	Electrical measurements: EIS	(Maoz et al., 2017)
	Kidney	Electric measurements: EIS	(Choudhury et al., 2022; Shaughnessey et al., 2022)
Spheroid size	Cancer and cardiac spheroids in hanging-drop networks	Electrical measurement: EIS	(Schmid et al., 2016)
Cell viability	Cardiomyocytes, HeLa cells	Electrical measurements: ECIS	(Wei et al., 2019)
Cell adhesion	Endothelial cells	Electromechanical sensor: QCM	(Marx et al., 2001)
Cell morphology, motility, and tracking	Fibroblasts, HepG2 cells	Optical measurement: mini-microscope	(Kim et al., 2012; Zhang et al., 2015)
Electrophysiology	Neurons	Electrical measurements: EFP	(Bruno et al., 2020)
	Cardiomyocytes, HeLa	Electrical measurements: EFP	(Wei et al., 2019)
Temperature	Blank OoC	Electrical sensor: CMOS-integrated PTAT current generator	(da Ponte et al., 2021)
	Three-dimensional Tumor	Electrical sensor: Integrated T-type thermocouple + Thermochromic film	(Zervantonakis and Arvanitis, 2016)
	HepG2, H1975, and Hepatic stellate cells	Electrical sensor: Integrated thin-film Pt resistance thermometer	(Zhao et al., 2021)
Mechanical strain/ contraction	Heart	Electromechanical sensor: Piezoelectric microcantilever	(Sakamiya et al., 2020)
	Heart	Optical sensor: Piezoelectrically actuated microcantilever	(Caluori et al., 2019; Coln et al., 2019)

(*continued on next page*)

Table 1 (*continued*)

Biomarker/target signal	Model	Detection method	References
	Heart	Electrical sensor: flexible strain gauge provides continuous and non-invasive readout of contractile stress and beat rate	(Lind et al., 2017)
	Heart	Optical measurement: Contraction force estimated by wire deflections	(Zhao et al., 2020)
	Heart	Optical measurement: Contraction force estimated by probe displacement	(Sidorov et al., 2017)
	ALS	Optical measurement: Contraction force estimated by pillar displacement	(Osaki et al., 2018)
Oxygen	Heart	Optical sensor: Luminescence (Oxygen quenching)	(Azizgolshani et al., 2021; Matsumoto et al., 2018; Rennert et al., 2015; Schneider et al., 2022)
	Heart, Brain cancer, Breast cancer	Electrochemical sensor: Amperometric	(Dornhof et al., 2022; Tanumihardja et al., 2021; Weltin et al., 2014)
pH	Heart, Brain cancer	Electrochemical sensor: Potentiometric	(Tanumihardja et al., 2021; Weltin et al., 2014)
	Lung cancer, Liver	Optical sensor: Absorbance (Phenol red)	(Khalid et al., 2020)
ROS/RNS	Human mammary fibroblasts and MCF-7	Optical sensor: Oxidant-sensitive dye fluorescence	(Zuchowska et al., 2018)
	Macrophages	Electrochemical sensor: Amperometric	(Li et al., 2018)
Lactate and glucose	Breast cancer, Liver	Electrochemical sensor: Amperometric enzymatic	(Dornhof et al., 2022; Weltin et al., 2017)
	Brain cancer	Electrochemical sensor: Amperometric enzymatic	(Weltin et al., 2014)
Glutamate	Brain	Electrochemical sensors: Amperometric enzymatic	(Nasr et al., 2018)
Insulin	Pancreas	On-line Optical sensor: SPR	(Ortega et al., 2021)
	Pancreas	Off-line Optical measurement: Raman	(Zbinden et al., 2020)
CK-MB, Troponin T, and HER-2	Heart-breast cancer	Off-line Electrochemical sensor: Faradaic EIS	(Lee et al., 2021)
CK-MB, Albumin, and GST-α	Live heart	On-line Electrochemical sensor: Faradaic EIS	(Zhang et al., 2017)
IFN-γ and TNF-α	CD4 and U937 cells	Electrochemical: Amperometric aptasensor	(Liu et al., 2015; Zhou et al., 2014)
IFN-γ and IL-2	Primary T lymphocytes	Optical sensor: SPR	(Baganizi et al., 2015)
IL-4, IL-6, IL-10, and TNF-α	Adipose tissue	Optical sensor: SPR	(Zhu et al., 2018)
TGF-β1	Liver	Electrochemical sensor: Amperometric aptasensor	(Matharu et al., 2014; Zhou et al., 2015)
HGF and TGF-β1		Optical sensor: Fluorescent immuno-microbeads	(Son et al., 2017)
IL-6 and TNF-α	Muscle	On-line Electrochemical sensor: Amperometric ELISA	(Ortega et al., 2019)
Architectural changes	Synovium	Optical measurement: Light scattering	(Rothbauer et al., 2020)

ALS: Amyotrophic lateral sclerosis; BBB: Blood–brain barrier; ECIS: Electric cell-surface impedance sensing; EFP: Extracellular field potentials; EIS: Electrochemical impedance spectroscopy; ELISA: Enzyme-linked immunosorbent assay; PTAT: Proportional to absolute temperature; QCM: Quartz crystal microbalance; ROS/RNS: Reactive oxygen species/Reactive nitrogen species; SPR: Surface plasmon resonance

determine the optimal culture conditions for recapitulating the physiological gut barrier function (Bossink et al., 2021; Henry et al., 2017; Jeon et al., 2022) and modeling the dysfunctions in the gut barrier caused by external factors (Jeon et al., 2022). Recently, microfluidic gut-on-a-chip containing human gut epithelium co-cultured with microbes has been established, and gut barrier protection by probiotics has been examined in this device by integrating it with gold electrodes (Jeon et al., 2022). The gut-on-a-chip exhibited a sharp decrease in barrier integrity in the presence of lipopolysaccharides (LPSs) and slow recovery of barrier function within 4 h of treatment with a probiotic strain (Jeon et al., 2022). Interestingly, the approach to calculate TEER on a chip has also been used to investigate the effects of microvariations in strain on lung alveolar barrier integrity, showing the how mechanical input induces the change of junctional complexes in lung model (Mermoud et al., 2018). The abovementioned findings reveal the robustnesses of OoCs integrated with TEER-monitoring devices for the investigation of tissue barrier formation, dynamics, and dysfunction.

5.1.2. Size of the tissue construct

Spheroids are spherical clusters of cell cultures that are used for biological research, specifically for cancer studies (Han et al., 2021). Several evidences have demonstrated that spheroids more accurately mimic tumor behavior than 2D cell cultures because of more realistic cell–cell interactions and a hypoxic gradient. Therefore, spheroid technologies have also been applied to develop cancers-on-chips with better pathological relevances (Bērziņa et al., 2021). The sizes of spheroids are

one of the critical parameters affecting drug penetration and cellular responses. Larger-sized spheroids or organoids are capable of sustaining oxygen and nutrient gradients, which forms a necrotic core found in poorly vascularized tumors *in vivo* (Ro et al., 2022). OoCs can improve the uniformities of the microstructures of 3D models (Moshksayan et al., 2018; Wu et al., 2022); nevertheless, the monitoring and analysis of spheroid sizes are impeded by methodological limitations. Schmid et al. proposed the integration of electrochemical impedance spectroscopy (EIS) readout function into spheroid platform as a label-free and non-invasive spheroid size analysis method (Schmid et al., 2016) (Fig. 4A). This approach was adopted to record the contraction and relaxation cycle of the beating rate of a cardiac spheroid and can be further employed for automated drop height control to achieve robust spheroid culture in OoCs.

5.2. Physical factors

5.2.1. Temperature

Temperature affects various properties, including structure and permeability, of the cell membrane (Quinn, 1988). Extremely high or low temperatures can cause serious damage to cells and even induce cell death (Quinn, 1988). Most cells function best at normal body temperature, which is approximately 37 °C (Ham and Puck, 1962; Kattipparambil Rajan et al., 2017); however, some cells demonstrate better functionalities at different temperatures depending on the tissue environment. For example, the differentiation of keratinocytes more efficiently occurs at temperatures lower than 37 °C because native skin cells are exposed to 32 °C on the skin surface (Frese et al., 2021). To recapitulate the physiological functions of cells on chips, determining the optimal temperature for each stage of cell culture and controlling the temperature constant in a closed system are essential. A recent study has explored the monolithic integration of a complementary metal oxide semiconductor with a polydimethylsiloxane OoC to sense the temperature of the cell medium in the OoC (da Ponte et al., 2021). This platform enabled real-time monitoring of the temperature of the cell medium with an accuracy of 0.2 °C (da Ponte et al., 2021). This approach can also be applied to investigate the efficacy of heat-driven drug release in cancer therapy. Single-channel brain cancer-on-a-chip was integrated with a temperature sensor and a focused ultrasound (FUS) system as a heat inducer. This platform facilitated the assessment and quantification of drug transport modulation by FUS in solid tumors (glioblastomas) (Zervantonakis and Arvanitis, 2016). The real-time monitoring of temperature enabled fine-tuning of the amplitudes of the FUS waves for appropriate temperature control in the OoC. Using this OoC setup, it was observed that FUS increased the temperature to an optimal range and thus triggered the local release of doxorubicin from a liposomal carrier, resulting in cell death in the FUS focal region (Zervantonakis and Arvanitis, 2016) (Fig. 4B).

5.2.2. Cell mechanical forces

Physiologies of the contractions of cardiac and skeletal muscles are similar (Boys and Owens, 2021). Muscle dysfunction significantly reduces the quality of life and even leads to death because muscle tissues play pivotal roles in physical activity, the movements of internal organs,

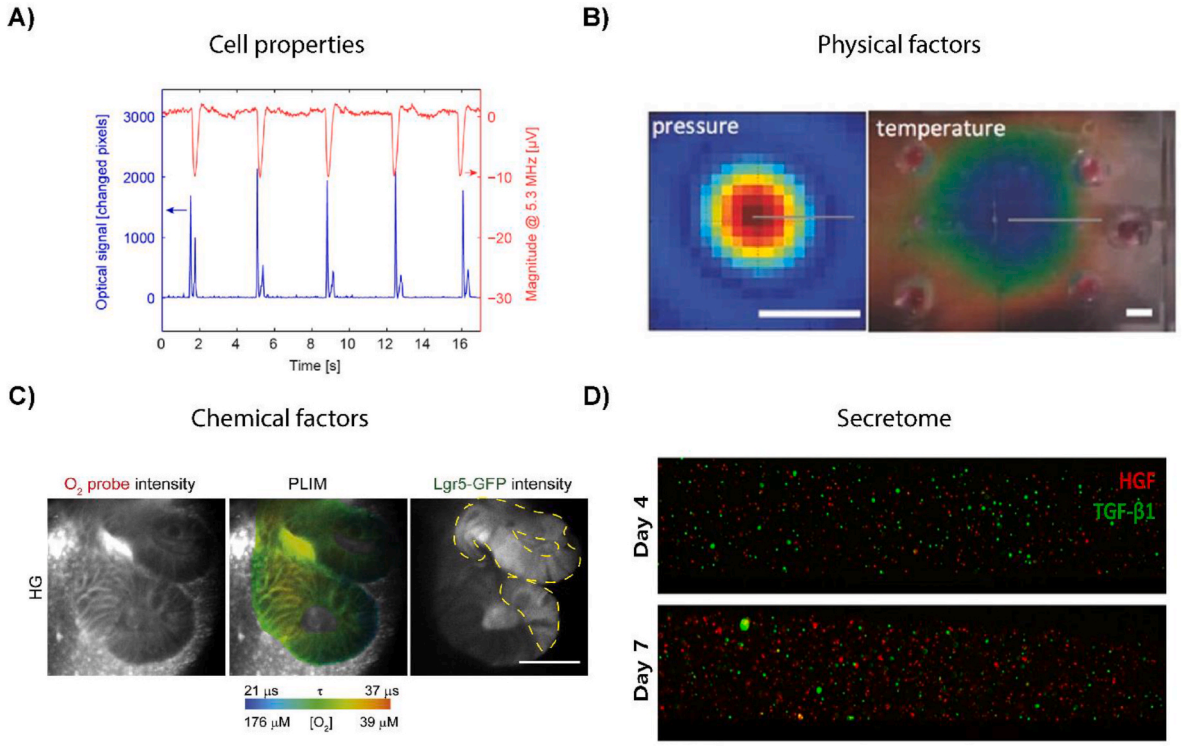

Fig. 4. Monitoring of physical, chemical, and biochemical parameters and cellular morphology within OoCs. **A)** Changes in the sizes (namely, cellular morphologies) of human cardiac microtissue (hCdMT) spheroids were examined by electrical impedance spectroscopy as a label-free and non-invasive analysis method. Electrodes measured the sizes of the tumor spheroids, beating frequencies and contraction-relaxation cycles of the cardiac spheroids (Schmid et al., 2016). **B)** Temperature and pressure (physical parameters) were evaluated using a hydrophone and thermochromic film of the focused ultrasound (FUS) focal region on a three-dimensional (3D) tumor platform (Zervantonakis and Arvanitis, 2016). **C)** Nicotinamide adenine dinucleotide phosphate (NAD(P)H) and real-time oxygenation (chemical parameters) were monitored via fluorescence lifetime imaging microscopy (FLIM) and phosphorescence lifetime imaging microscopy (PLIM), respectively. Lifetime imaging was measured luminescence through microscopy in intestinal organoids (Okkelman et al., 2020). **D)** Hepatocyte growth factor (HGF) and transforming growth factor (TGF)-β1 (biochemical parameters) in primary hepatocytes within a microfluidic device were detected using fluorescent microbead-based sensors and measured via microscopy (Son et al., 2017). Panel A is reproduced with permission from Schmid et al. (2016). Copyright 2016 American Chemical Society. Panel B is reproduced with permission from Zervantonakis and Arvanitis (2016). Copyright 2016 John Wiley and Sons. Panel C is reproduced with permission from Okkelman et al. (2020). Copyright 2020 Elsevier. Panel D is reproduced with permission from Son et al. (2017). Copyright 2017 Springer Nature.

and the pumping of blood throughout the body. As the number of muscular system diseases is increasing worldwide, a better understanding of the mechanisms of muscle pathologies to guide the development of drugs that resolve the underlying causes is urgently needed (Ajalik et al., 2022). OoCs that recapitulate cardiac or skeletal muscular pathologies require a sensitive monitoring system that can quantify muscle contraction as an indicator of muscle activity (Dou et al., 2022). Amyotrophic lateral sclerosis (ALS) is a neurodegenerative disease in which motor neuron loss in the spinal cord and motor cortex causes muscle atrophy (Osaki et al., 2018). Because the genetic factors underlying ALS are still unknown, an ALS model generated using patient-derived iPSCs can serve as a promising *in vitro* tool for the analysis of the related mechanism.

To investigate how motor neurons with different genetic mutations affect muscle activity, Osaki et al. (2018) developed iPSC-derived ALS-on-a-chip integrated with a module for the imaging-based detection of muscle activity. Monitoring the deflections of soft pillars fabricated in a microchannel and further image analysis enabled the quantification of the contractile behaviors of the muscles attached to the pillars and examination of the effect of an ALS drug (Osaki et al., 2018).

Half of all drugs withdrawn from the market in the last 30 years have caused cardiac muscle damage, which indicates the urgent need for heart models for reliable and robust cardiotoxicity tests. Sakamiya et al. (2020) developed heart-on-a-chip containing cardiac muscle fibers with higher robustness in the measurement of muscular contraction by a piezoelectric sensing system, similar to the approach used to monitor the deflections of pillars (Osaki et al., 2018).

Another study proposed embedding a sensor based on microcracked gold thin films in heart-on-a-chip, which was deformed by the stress exerted by cardiac tissue overlaid on the sensor (Lind et al., 2017). This platform facilitates continuous and non-invasive readout of the contractile stress and thus can be used for a rapid cardiotoxicity test (Lind et al., 2017). The abovementioned hearts-on-chips integrated with contraction-monitoring devices would serve as significant tools for the investigation of the cardiotoxic effects of the drugs transformed by other organs, such as liver and intestine, in a complex multi-organ platform.

5.2.3. Electrophysiology

The activity of electrogenic cells generate a complex voltage signal composed of a lower frequency fluctuation, the local field potential, and high frequency spikes (Buzsáki et al., 2012). This local field potential is generated during the collective and synchronous synaptic input, and the spikes are action potential bursts, which are transient changes in individual cell membrane potentials that rise and fall rapidly in the spaces outside electrogenic cells as a result of their normal activity (Hodgkin and Huxley, 1952). Electrophysiological activity recordings of extracellular field potentials permit close scrutiny of the behavior and function of the cellular network and disorders in the cellular network. For neurons, action potentials are related to synaptic transmission and postsynaptic glutamate receptors, whereas for cardiac cells, electrical activity is associated with normal cardiac function in terms of rate, rhythm, and initiation of cardiac muscle contraction (Kléber and Rudy, 2004). In pancreatic islet β-cells, the electrical activity is induced by glucose intake, which also triggers insulin secretion (MacDonald and Rorsman, 2006).

Bruno et al. (2020) used a microfluidic setup to deliver caffeine in a spatially localized manner to primary hippocampal and cortical neurons seeded on microelectrode arrays. Simultaneous recordings of the extracellular field potentials of the neural network directly correlated the intake of caffeine with an increased electrophysiological activity. Similarly, Wei et al. (2019) employed a microfluidic device to evaluate the cardiotoxicities of two anticancer drugs based on the electrophysiologies of cardiomyocytes.

5.3. Chemical factors

5.3.1. Oxygen

Oxygen is an important modulator of cellular function in both normal and disease states, affecting cell growth and differentiation and enzyme expression. In standard cell cultures, oxygen tension is controlled by adjusting the concentration of gas in the incubator (Freshney, 2010a). In contrast, in OoCs, oxygen is supplied through OoCs, whereas in dissolved form, it is delivered via the perfusing media, which renders the regulation of oxygen levels in OoCs more complex. Thus, the integration of oxygen sensors into OoCs has been of particular interest for oxygen-input control and measuring the output oxygen concentration, indicating oxygen consumption by cells (Azizgolshani et al., 2021; Figueiredo et al., 2020; Jalili-Firoozinezhad et al., 2019; Matsumoto et al., 2018; Moya et al., 2018; Rennert et al., 2015; Tanumihardja et al., 2021). Specifically, real-time assessment of physiologically relevant oxygen gradients is critical to establish an OoC recapitulating an anaerobic gut environment. Due to intense microbial metabolic activity, oxygen levels in the gut remain low (~5%); accordingly, the majority of the human gut microbiome comprises obligate anaerobic bacteria (Zeitouni et al., 2016). Jalili-Firoozinezhad et al. (2019) proposed gut-on-a-chip integrated with an oxygen sensor (VisiSens system), where measurements were conducted by non-invasive fluorescence readout to monitor the oxygen concentration in real time. The gut platform demonstrated improved intestinal barrier function and microbial diversity in transluminal hypoxic gradients as compared to those in the cases of aerobic co-culture systems, suggesting the importance of oxygen input in modeling the host–microbiome interactions (Jalili-Firoozinezhad et al., 2019). Furthermore, the oxygen sensor integrated into the OoC served as a tool for the evaluation of the oxygen consumption rates of cells, which indicate mitochondrial function in response to biochemical or mechanical stimuli. Particularly, the heart operates solely under aerobic metabolism; thus, myocardial mitochondria maintain an abundance of oxygen to continue oxidative phosphorylation. To examine the functional activity of engineered myocardium *in vitro*, several hearts-on-chips have been integrated with luminescent optical oxygen-monitoring systems (Azizgolshani et al., 2021; Matsumoto et al., 2018; Rennert et al., 2015; Schneider et al., 2022) and electrochemical sensing systems (Tanumihardja et al., 2021) and used to test the cardiotoxicities of drugs. As a different approach, oxygen consumption and heterogeneity of organoid oxygenation in a gut organoid platform were assessed using phosphorescence lifetime imaging microscopy (PLIM) (Okkelman et al., 2020). Phosphorescence of a small-molecular oxygen probe (Pt-Glc), which selectively stained epithelial cells, was specifically quenched by molecular oxygen and imaged by PLIM, allowing oxygen monitoring in specific cell types (Fig. 4C). The suggested PLIM approach appears promising for sensing oxygen levels in OoCs with 3D tissue constructs, such as organoids, composed of multiple cell types (Okkelman et al., 2020).

5.3.2. pH

Although most cells appropriately function at pH = 7.4, the optimal pH for cell growth varies among cell types (Freshney, 2010b). Maintaining a suitable pH is vital for appropriate cellular activity; therefore, pH monitoring and control are essential for *in vitro* culture systems (Freshney, 2010b). In standard culture media, phenol red is used as a pH indicator to identify changes in pH from neutral (red) to acidic (yellow). Typically, a change in the color of phenol red to yellow indicates high glycolytic metabolic activities of the cells. Some OoCs, including liver-on-a-chip (Farooqi et al., 2020) and lung cancer-on-a-chip (Khalid et al., 2020), have been integrated with optical pH sensors to measure the variation in the light intensity of the perfusion culture media containing phenol indicators to monitor changes in cell metabolism. Both studies validated the pH sensor system by showing the pH decrease in the culture media as a result of proliferated cells in the OoC. Moreover, cancer drug-induced acidification was noticed in a lung cancer model

using an optical pH sensor (Khalid et al., 2020). Furthermore, integration of OoCs with potentiometric pH sensors based on ruthenium oxide (Tanumihardja et al., 2021) or electrodes formed by anodic electrodeposition of iridium oxide thin films (Weltin et al., 2014) has been proposed, and the resulting systems successfully detected altered cell metabolisms caused by drug treatments.

5.4. Metabolome

5.4.1. Metabolites

Metabolism is the sum of the biochemical processes in living organisms that either produce or consume energy (DeBerardinis and Thompson, 2012). Core metabolism involves pathways to process abundant nutrients, such as carbohydrates, fatty acids, and amino acids, essential for energy homeostasis and macromolecular synthesis in humans (DeBerardinis and Thompson, 2012). Dysregulation of cell metabolism is common in cancer, immunological disorders, obesity, diabetes, and neurodegenerative diseases. Dynamic monitoring of cell metabolism in OoC facilitates the investigation of cellular bioenergetics at the tissue level, which provides valuable insights into the disease, environmental effects on metabolism, and drug target discovery (Bavli et al., 2016; Kemas et al., 2021; Maioli et al., 2016; Misun et al., 2016; Obregón et al., 2013). Dornhof et al. (2022) recently proposed breast cancer-on-a-chip that enables *in situ* electrochemical sensing of glucose and lactate in real time. In cancer cells, glucose uptake is considerably high owing to the reprogrammed metabolic pathway, and accordingly, the secretion of lactate as a waste product is increased. Thus, measurement of glucose and lactate levels in spent media reveals the metabolic activities of cancer cells in OoC (Dornhof et al., 2022). Electrochemical sensors were fabricated by sequential UV curing of poly(2-hydroxyethyl methacrylate) (pHEMA) with entrapped lactate oxidase and glucose oxidase dispensed onto an electropolymer membrane. Detection of glucose and lactate from the media was based on the equimolar conversions of glucose and lactate into H_2O_2 inside the pHEMA-based hydrogel, and the concentrations of glucose and lactate were determined by the current density for H_2O_2 oxidation. Considering that aerobic glycolysis and lactate secretion have emerged as important therapeutic targets, the proposed platform can be employed to discover new metabolic cancer treatments. Nevertheless, the levels of metabolites can be indicators of the maturation and functionality of the tissue model. Glutamate is a primary metabolite in the central nervous system and functions as an excitatory neurotransmitter (Zhou and Danbolt, 2014). It plays a central role in cognitive functions, for example, synaptic plasticity and neural network formation (Zhou and Danbolt, 2014); thus, glutamate levels in brain models imply neuronal maturation and activity *in vitro*. Brains-on-chips embedded with electrochemical biosensors to monitor glutamate have been proposed for neurodevelopmental studies (Nasr et al., 2018). However, there are large numbers of metabolites in humans (approximately 220,000) (Wishart et al., 2022), and technologies to detect and quantify various metabolites in real time are still lacking. Technological progresses in continuous sensing of metabolites in OoCs would significantly advance the OoC field.

5.4.2. Reactive oxygen species (ROS) and reactive nitrogen species (RNS)

ROS are continuously produced in animals as by-products of aerobic metabolism and kept in balance with the antioxidant defense systems. Some ROS act as secondary messengers in cellular signaling; they are essential for numerous biological processes (Schieber and Chandel, 2014; Sinenko et al., 2021), as well as play a role in the aging process (Santos et al., 2018). Nevertheless, an increase in ROS levels as a result of oxidative stress can cause damage cell biomolecules such as nucleic acids, proteins, and membrane lipids, leading to a variety of diseases (Schieber and Chandel, 2014; Sinenko et al., 2021). Therefore, in several cell-related fields including oncology, drug development, and tissue engineering, a technique capable of monitoring ROS *in situ* in real time is required. Despite the difficulties in measuring the ROS levels, many methods for ROS level measurement have been reported in the literature such as fluorescent and chemiluminescent probe-based methods, spectrophotometry, spectroscopy, and chromatography (Griendling et al., 2016; Sharma et al., 2017). However, a platform for the non-invasive monitoring of cell culture-secreted ROS is still lacking. Li et al. (2018) proposed an innovative microfluidic platform for the electrochemical monitoring of ROS and RNS. The proposed platform consisted of an upstream microchamber for cell culture and four parallel microchannels located downstream for the separate detection of H_2O_2, $ONOO^-$, $NO\cdot$, and NO_2^-. Amperometric measurements of ROS and RNS levels were performed using high-sensitivity platinum-black electrodes embedded in microchannels (Li et al., 2017). Results indicated increased levels of the abovementioned chemicals in macrophages in the presence of calcium ionophores (Li et al., 2017). In another study, the ROS levels were examined by intensity measurements using the oxidant-sensitive dye 2′, 7′-dichlorofluorescin diacetate in breast cancer-on-a-chip (Zuchowska et al., 2018). The platform was utilized to successfully analyze the efficacy of photodynamic therapy by observing the increase of ROS levels in cancer cells undergoing cell death.

5.5. Secretome

Proteins secreted by human cells are crucial for not only the basic understanding of human biology, but also the identification of potential targets for future therapies. Moreover, many of these proteins, for instance, cytokines, growth factors, and hormones, are both locally and systemically involved in signaling functions. Cells exhibit dynamic secretome profiles according to their type, characteristics, developmental processes, cancer progression (da Cunha et al., 2019), and environmental exposure (Uhlén et al., 2019). Thus, quantitative detection of secretome biomarkers is important to understand the biological and pathological processes occurring in OoCs (Kilic et al., 2018).

5.5.1. Cytokines

Cytokines are small secreted proteins that are key modulators of inflammation. Measurement of cytokine concentration is critical for monitoring infections, disease processes, and cytotoxicities in OoCs, which mimic (patho)physiological microenvironments (Li et al., 2017; Ortega et al., 2019; Shin et al., 2016; Son et al., 2017; Zhou et al., 2015; Zhu et al., 2018). To detect cytokines in OoCs, several protein-sensing systems, such as electrochemical aptasensors (Liu et al., 2015; Matharu et al., 2014; Zhou et al., 2014, 2015), optical sensors based on SPR (Baganizi et al., 2015; Zhu et al., 2018), and functionalized beads (Son et al., 2017), and protein-sensing techniques, including amperometric ELISA (Ortega et al., 2019), have been suggested (Fig. 4D). Recently, microfluidic adipose-tissue-on-chip integrated with a localized SPR (LSPR)-based optical biosensor was proposed by Zhu et al. (2018), which enabled *in situ*, real-time, label-free, and high-throughput analysis of cytokines. In obesity, altered cytokine profiles secreted from adipose tissues result in the recruitment of immune cells and further inflammation-induced metabolic disorders. Thus, simultaneous measurements of pro-inflammatory (interleukin (IL)-6 and tumor necrosis factor (TNF)-α) and anti-inflammatory (IL-10 and IL-4) cytokines by antibody-conjugated sensor arrays in adipose tissue-on-chip can be useful tools for monitoring adipose progression and discovering obesity treatment strategies. Furthermore, IL-6 and TNF-α were detected in skeletal muscle-on-a-chip via amperometric ELISA (Ortega et al., 2019). Functionalized high-sensitivity screen-printed gold electrodes were linked to this OcC via tubing, and cytokine levels in the perfusing media containing secretome of muscle tissue were evaluated outside the OoC. By measuring cytokines, this platform revealed the inflammatory induction in the muscle tissue in response to electrical signals and LPS (Ortega et al., 2019).

5.5.2. Biochemical markers of organ function

Detection of biochemical markers, such as insulin, creatine kinase

MB (CK-MB), troponin T, albumin, and glutathione S-transferase α (GST-α), which represent organ function, has facilitated the determination of the risks of various diseases and the health status of an individual. This approach can also be applied to OoCs to evaluate their cellular functions, investigate drug-induced cytotoxicity, and model diseases. For example, the level of secreted insulin can define the functions of pancreatic β-cells in islet-on-a-chip. To continuously monitor insulin secretion, LSPR biosensing modules (Ortega et al., 2021) and Raman spectroscopy (Zbinden et al., 2020) have been introduced into the pancreas-on-a-chip in individual studies as optical measurement tools. Considering that a decrease in the insulin level is a key pathological event in metabolic disorders, these platforms can be utilized to model the pathological environment in type 2 diabetes and discover therapeutic strategies. In contrast, cardiac troponin T and CK-MB are sensitive biomarkers for assessing cardiac damage in clinical practice and are extensively employed in drug safety assessment; therefore, integration of sensors that can detect these markers into heart-on-a-chip can facilitate a robust cardiotoxicity test (Aleman et al., 2021; Lee et al., 2021). Lee et al. (2021) proposed an OoC containing heart and breast tumor tissues integrated with an electrochemical aptasensor to monitor troponin T and CK-MB levels. This platform was used to investigate differences between the functionalities of healthy and fibrotic cardiac tissues following treatment with a breast cancer chemotherapeutic agent. Similarly, hepatotoxicity was continuously examined by evaluating the levels of albumin and GST-α in liver-on-a-chip using electrochemical affinity-based biosensors integrated into the liver-on-a-chip (Zhang et al., 2017).

6. Future perspectives

Integration of biosensors into OoCs for the real-time, continuous, and long-term monitoring of biomarkers in cell media is a challenging goal that is currently hampered by the following limitations: i) passivation of biosensor surfaces for long-term monitoring due to biofouling, ii) saturation of the biosensor surface owing to inherent thermodynamic and kinetic limitations of bioreceptors, and iii) label and reagent requirements for the detection of most bioanalytes.

Biofouling refers to the non-specific adsorption of biological substances on a surface in direct contact with a complex matrix containing high concentrations of proteins such as plasma and cell media. Performances of electrochemical biosensors substantially decrease because of the electrical passivation of their surfaces. Moreover, all biosensing strategies, particularly label-free strategies, are susceptible to false positives. The output signals obtained via SPR or EIS sensors for specifically bound target analytes are indistinguishable from those acquired for other adsorbed interferents. Numerous strategies have been reported to limit non-specific adsorption on biosensor surfaces and surface passivation of these surfaces that occur when these surfaces come in direct contact with complex media (Jiang et al., 2020). Nevertheless, these approaches typically rely on the formation of antifouling coatings, which, as a double-edged sword, also limit the sensitivity of the biosensing surface. Recently, we developed a simple coating for biosensors using highly porous cross-linked bovine serum albumin that prevented sensitivity loss owing to biofouling in plasma for over a month, and the coated electrochemical biosensors retained $>$ 90% of their original sensitivities (Sabaté del Río et al., 2019). Although this antifouling method proved effective, we further extended this idea for generating nanostructured and nanoporous gold surfaces to prevent biofouling and simultaneously increase the sensitivities of our assays and detect analytes at small concentrations in complex media (Sabaté del Río et al., 2022).

Surface saturation is an inherent limitation of current biosensing technologies for real-time and continuous monitoring because traditionally, the biosensing field has been considerably established for endpoint diagnostic assays. The use of single-point sampling of OoC for traditional off-chip detection and analysis, including mass spectrometry, staining techniques, flow cytometry, and microfluorimetry, is one of the strategies to overcome the abovementioned limitation. Other strategies used to overcome this limitation employ on-line modular microfluidic chips for biosensing. Using microvalves and pumps, a full assay can be programmed and autonomously run on a different chip. For instance, a single-cell barcode chip is an analytical device capable of high-throughput multiplex biomarker analysis via spatially encoded antibody barcodes (Ma et al., 2011; Tak For Yu et al., 2015). In another potential strategy, these modular microfluidic chips are utilized to dissociate bioreceptor–target binding after being saturated with mild reagents (Goode et al., 2015); however, the performances of the biosensors decrease after each cycle due to the denaturation of bioreceptors. In this regard, a full electrode surface regeneration protocol has been proposed to prevent the loss of the performances of biosensors after each regeneration. The concept is based on a dual-step cleaning protocol that allows up to a total of five measurements in a modular setup containing OoCs (Aleman et al., 2021; Zhang et al., 2017). A very promising approach in this regard is the use of disposable magnetic microbeads that can be functionalized with specific bioreceptors, incubated into the OoC to capture the analytes of interest, and analyzed in a different microfluidic chip by fixing them with an external magnetic field. This is a versatile strategy that enables the detection of multiple targets on demand, and because the beads are replaced after each use, multiple measurements are possible (Riahi et al., 2016). Nevertheless, these surface regeneration strategies are intrinsically limited by bioreceptor saturation during on-chip continuous monitoring based on affinity interactions and are not viable because of cell damage. Biomolecular bioreceptor–target interactions are inherently restricted by the trade-off between thermodynamics and kinetics. This indicates that if bioreceptors with high sensitivities are used, the trade-off is that at low target concentrations, the equilibrium state where detection can be performed will be achieved after a long time. An interesting idea to overcome this limitation is the hypothetical use of pre-equilibrium biosensing, a detection technique based on the measurement of real-time changes in target concentrations prior to target–receptor equilibration using frequency domain analysis rather than the traditional time domain analysis (Maganzini et al., 2022).

In contrast, for the detection of many important biomarkers, affinity-based strategies are needed, which generally require labels and reagents to yield optical or electrochemical signal outputs. This implies that these biosensing strategies cannot be integrated on-chip because the reagents and washing steps may affect and damage the cells. The most promising strategy to overcome this limitation is the use of aptamers, which not only exhibit high chemical stabilities upon regeneration, but can also be labeled with electroactive molecule reporters to realize reagent- and wash-free detection of protein biomarkers (Clifford et al., 2021). In this strategy, the binding between the bioreceptor and the target leads to a conformational change of the bioreceptor, ultimately changing the electron transfer kinetics between the electroactive reporter and the surface of the electrode. This strategy has been employed with impedance measurements to avoid common false positives because the signal output originates from the phase shift of the current instead of changes in the electrode surface (Downs et al., 2020). In similar approaches, DNA scaffolds, protein scaffolds, protein folding, and molecular pendulums have been used (Clifford et al., 2021).

7. Summary and conclusions

OoCs emulate an organ via microfluidic cell culture and demonstrate physiological and key functional traits of that organ. To develop an OoC, controlling the physicochemical stimuli on the chip is important to mimic the microenvironment of the original organ. Furthermore, evaluating whether the functions of OoC tissues or cells represent the *in vivo* functions of the organ is necessary. OoCs have the potential to reduce the use of animal models in drug studies, replace traditional 2D cell cultures due to their higher physiological relevance, and open up new

avenues for drug screening and personalized medicine. Despite extensive development, the reliabilities, reproducibilities, and representativeness of these models for physiological, pathological, and pharmacological studies still need to be examined. In addition to issues associated with the inadequate fabrication scalabilities of these models, high-throughput assays are required to obtain robust data and models for clinical studies. To address these issues, a viable solution is to miniaturize, adapt, and directly integrate monitoring techniques and devices into the OoC such that analytical information can be continuously and non-invasively obtained *in situ* in real time. These data are necessary at different stages of the OoC workflow: to ensure appropriate chip development and obtain consistent batch-to-batch OoC during the development of an OoC; to regulate the OoC status and maintain homeostasis before the assay; and finally, to provide strong correlation between an external test stimulus and the outcome of the assay during the assay.

Traditional monitoring methods utilize invasive off-chip end-point assays that fail to afford the spatiotemporal resolution required to characterize the dynamic processes involved in cell physiology and only provide delayed information on the events occurring in the OoC. To date, although only few detection schemes and sensing modalities have been integrated with OoCs, even in these cases, the integration of monitoring devices is more an addition to justify certain hypotheses. To validate the use of OoC and advance this technology, specifically in the pharmaceutical industry, the implication of multiplex biosensing technologies cannot be an afterthought, but a key feature of the design. To date, only a few sensors have been widely integrated with OoCs to enable continuous and real-time monitoring of oxygen, pH, temperature, flow rate, and some metabolites, for instance, glucose and lactate. These parameters are important for regulating physicochemical stimuli and cell metabolism; however, most of the cell secretome and other markers, including extracellular vesicles and ROS, related to cell signaling and biochemical parameters associated with medium composition and cell physiology and functionality are still unexplored. Off-line traditional analytical tools are still crucial for the analysis and characterization of genomes and transcriptomes; nevertheless, they cannot capture the dynamic cell behavior with sufficient time resolution. Incorporating a ribonucleic acid (RNA)-detection or -sequencing tool into OoCs would be advantageous because transcriptomes have more dynamic profiles than those of genomes and play important roles in the cell signaling pathway. However, integration of RNA-detection or -sequencing tools into OoCs is extremely challenging.

The remaining challenges for the integration of real-time and continuous biosensing techniques into OoCs are biofouling, surface passivation, bioreceptor saturation, and the lack of appropriate label-free and reagent-free detection techniques. Some ideas for overcoming these limitations include the use of antifouling surfaces, aptamers, single-cell barcodes, and cell-free transcription factor-based biosensors

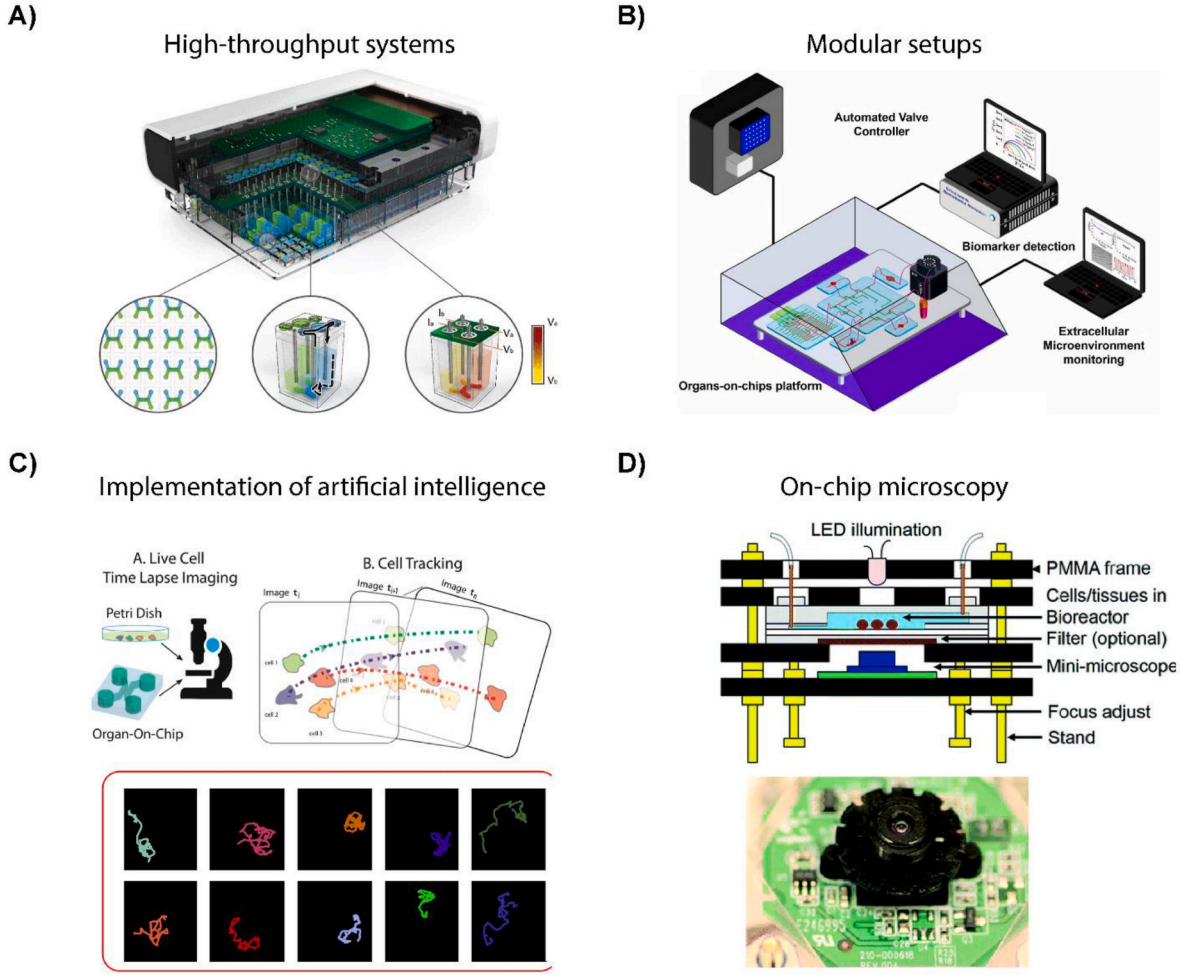

Fig. 5. Future perspectives for biosensor-integrated OoCs. **A)** To develop biosensor-integrated OoCs, high-throughput systems (Azizgolshani et al., 2021), **B)** modular setups (Zhang et al., 2017), **C)** artificial intelligence (Mencattini et al., 2020), and **D)** on-chip microscopy can be integrated into OoCs (Zhang et al., 2015). Panel A is reproduced with permission from Azizgolshani et al. (2021). Copyright 2021 Royal Society of Chemistry. Panel B is reproduced with permission from Zhang et al. (2017). Copyright 2017 National Academy of Sciences. Panel C is reproduced with permission from Mencattini et al. (2020). Copyright 2020 Springer Nature. Panel D is reproduced with permission from Zhang et al. (2015). Copyright 2015 Royal Society of Chemistry.

for on-chip approaches, bead-based assays or surface regeneration protocols for on-line approaches, and novel transduction mechanisms. Only when this is achieved, multiplex real-time and continuous detection of biomarkers can be combined with deep learning algorithms for closed-loop feedback optimization and control for higher reliability and physiological resemblance of OoCs. OoCs are also facing another big challenge regarding fabrication scalability as high-throughput data acquisition is necessary for drug screening and profiling and pharmacokinetic evaluation (Fisher et al., 2022). At present, researchers should consider these requirements while designing future OoCs, adapting OoC preparation protocols, and using more appropriate raw materials. Design features such as plug-and-play functionality, modular designs for flexible prototyping, and simple integration of OoCs with commercially available sensors, materials, or actuators should be considered. Some excellent examples in this regard are miniaturized and integrated OoCs for high-throughput assays (Azizgolshani et al., 2021; Gard et al., 2021) (Fig. 5A). Additionally, replacement of the current off-line monitoring strategies with on-chip integrated biosensors will probably require the use of on-line microfluidic routing with modular lab-on-a-chip solutions (Miyazaki et al., 2021; Zhang et al., 2017) (Fig. 5B). Moreover, the current use of deep learning algorithms for cell tracking and identification and image segmentation (Li et al., 2022) (Fig. 5C) indicates promising future applications of artificial intelligence for the realization of cyber-physical systems. The integration of mini-microscopes (Kim et al., 2012; Takehara et al., 2017) (Fig. 5D) with artificial intelligence will probably be essential to parallelize multiple autonomous OoCs.

Despite significant progress in this field and all the pathophysiological knowledge acquired using OoCs, the establishment of this technology as a replacement for traditional 2D cell cultures and animal models in pharmacological studies is still debatable. To tackle this challenge, future OoC development requires a step forward in a new direction where biosensor integration is a fundamental part of the chip and "smart" cyber-physical systems using deep learning are the end goals. Only after this is achieved will we be able to extract, quantify, and correlate the relevant external stimuli in the microenvironment with the physicochemical response of the OoC. Therefore, future development of OoCs and other microphysiological systems will require extensive collaboration of multidisciplinary branches, including synthetic and molecular biology, artificial intelligence, and microfabrication, and eventually the consultancy of pharmaceutical companies and regulatory authorities.

Declaration of competing interest

The authors declare that they have no known competing financial interests or personal relationships that could have appeared to influence the work reported in this paper.

Data availability

No data was used for the research described in the article.

Acknowledgements

This work was supported by the funding received from the Institute for Basic Science (No. IBS-R020-D1), UNIST research grant 1.220023.01, and the National Research Foundation of Korea (NRF) grant (NRF-2022M3A91015716 and 2020M3H4A1A02084827) funded by the Korean government.

References

Ajalik, R.E., Alenchery, R.G., Cognetti, J.S., Zhang, V.Z., McGrath, J.L., Miller, B.L., Awad, H.A., 2022. Front. Bioeng. Biotechnol. 10, 846230.
Aleman, J., Kilic, T., Mille, L.S., Shin, S.R., Zhang, Y.S., 2021. Nat. Protoc. 16, 2564–2593.
Anik, Ü., Timur, S., Dursun, Z., 2019. Microchim. Acta 186, 196.
Anum Satti, J., Habib, A., Anam, H., Zeb, S., Amin, Y., Loo, J., Tenhunen, H., 2018. Int. J. RF Microw. Computer-Aided Eng. 28, e21151.
Apostolou, A., Panchakshari, R.A., Banerjee, A., Manatakis, D.V., Paraskevopoulou, M. D., Luc, R., Abu-Ali, G., Dimitriou, A., Lucchesi, C., Kulkarni, G., Maulana, T.I., Kasendra, M., Kerns, J.S., Bleck, B., Ewart, L., Manolakos, E.S., Hamilton, G.A., Giallourakis, C., Karalis, K., 2021. Cell. Mol. Gastroenterol. Hepatol. 12, 1719–1741.
Arık, Y.B., van der Helm, M.W., Odijk, M., Segerink, L.I., Passier, R., van den Berg, A., van der Meer, A.D., 2018. Biomicrofluidics 12, 042218.
Assimakopoulos, S.F., Triantos, C., Maroulis, I., Gogos, C., 2018. Gastroenterol. Res. 11, 261–263.
Azizgolshani, H., Coppeta, J.R., Vedula, E.M., Marr, E.E., Cain, B.P., Luu, R.J., Lech, M. P., Kann, S.H., Mulhern, T.J., Tandon, V., Tan, K., Haroutunian, N.J., Keegan, P., Rogers, M., Gard, A.L., Baldwin, K.B., de Souza, J.C., Hoefler, B.C., Bale, S.S., Kratchman, L.B., Zorn, A., Patterson, A., Kim, E.S., Petrie, T.A., Wiellette, E.L., Williams, C., Isenberg, B.C., Charest, J.L., 2021. Lab Chip 21, 1454–1474.
Badiola-Mateos, M., Di Giuseppe, D., Paoli, R., Lopez-Martinez, M.J., Mencattini, A., Samitier, J., Martinelli, E., 2021. Sensor. Actuator. B Chem. 334, 129599.
Baganizi, D.R., Leroy, L., Laplatine, L., Fairley, S.J., Heidmann, S., Menad, S., Livache, T., Marche, P.N., Roupioz, Y., 2015. Biosensors 5, 750–767.
Barmpakos, D., Kaltsas, G., 2021. Sensors 21, 739.
Bavli, D., Prill, S., Ezra, E., Levy, G., Cohen, M., Vinken, M., Vanfleteren, J., Jaeger, M., Nahmias, Y., 2016. Proc. Natl. Acad. Sci. USA 113, E2231–E2240.
Bērziņa, S., Harrison, A., Taly, V., Xiao, W., 2021. Cancers 13, 4192.
Białas, K., Moschou, D., Marken, F., Estrela, P., 2022. Microchim. Acta 189, 172.
Binder, A.R.D., Spiess, A.-N., Pfaffl, M.W., 2021. Sensors 21, 5286.
Booth, R., Noh, S., Kim, H., 2014. Lab Chip 14, 1880–1890.
Bossink, E.G.B.M., Zakharova, M., de Bruijn, D.S., Odijk, M., Segerink, L.I., 2021. Lab Chip 21, 2040–2049.
Boys, A.J., Owens, R.M., 2021. Apl. Mater. 9, 040903.
Bruno, G., Colistra, N., Melle, G., Cerea, A., Hubarevich, A., Deleye, L., De Angelis, F., Dipalo, M., 2020. Front. Bioeng. Biotechnol. 8, 626.
Buzsáki, G., Anastassiou, C.A., Koch, C., 2012. Nat. Rev. Neurosci. 13, 407–420.
Caluori, G., Pribyl, J., Pesl, M., Jelinkova, S., Rotrekl, V., Skladal, P., Raiteri, R., 2019. Biosens. Bioelectron. 124–125, 129–135.
Chalklen, T., Jing, Q., Kar-Narayan, S., 2020. Sensors 20, 5605.
Chen, C., Wang, J., 2020. Analyst 145, 1605–1628.
Chen, J.Y., Penn, L.S., Xi, J., 2018. Biosens. Bioelectron. 99, 593–602.
Chiu, D.T., deMello, A.J., Di Carlo, D., Doyle, P.S., Hansen, C., Maceiczyk, R.M., Wootton, R.C.R., 2017. Chem 2, 201–223.
Chou, D.B., Frismantas, V., Milton, Y., David, R., Pop-Damkov, P., Ferguson, D., MacDonald, A., Vargel Bölükbaşı, Ö., Joyce, C.E., Moreira Teixeira, L.S., Rech, A., Jiang, A., Calamari, E., Jalili-Firoozinezhad, S., Furlong, B.A., O'Sullivan, L.R., Ng, C.F., Choe, Y., Marquez, S., Myers, K.C., Weinberg, O.K., Hasserjian, R.P., Novak, R., Levy, O., Prantil-Baun, R., Novina, C.D., Shimamura, A., Ewart, L., Ingber, D.E., 2020. Nat. Biomed. Eng. 4, 394–406.
Choudhury, M.I., Li, Y., Mistriotis, P., Vasconcelos, A.C.N., Dixon, E.E., Yang, J., Benson, M., Maity, D., Walker, R., Martin, L., Koroma, F., Qian, F., Konstantopoulos, K., Woodward, O.M., Sun, S.X., 2022. Nat. Commun. 13, 2317.
Chung, M., Lee, S., Lee, B.J., Son, K., Jeon, N.L., Kim, J.H., 2018. Adv. Healthc. Mater. 7, 1700028.
Clifford, A., Das, J., Yousefi, H., Mahmud, A., Chen, J.B., Kelley, S.O., 2021. J. Am. Chem. Soc. 143, 5281–5294.
Coln, E.A., Colon, A., Long, C.J., Sriram, N.N., Esch, M., Prot, J.-M., Elbrecht, D.H., Wang, Y., Jackson, M., Shuler, M.L., Hickman, J.J., 2019. MRS Commun. 9, 1186–1192.
da Cunha, B.R., Domingos, C., Stefanini, A.C.B., Henrique, T., Polachini, G.M., Castelo-Branco, P., Tajara, E.H., 2019. J. Cancer 10, 4574–4587.
Das, R.S., Agrawal, Y.K., 2011. Vib. Spectrosc. 57, 163–176.
DeBerardinis, R.J., Thompson, C.B., 2012. Cell 148, 1132–1144.
Dornhof, J., Kieninger, J., Muralidharan, H., Maurer, J., Urban, G.A., Weltin, A., 2022. Lab Chip 22, 225–239.
Dou, W., Malhi, M., Zhao, Q., Wang, L., Huang, Z., Law, J., Liu, N., Simmons, C.A., Maynes, J.T., Sun, Y., 2022. Microsyst. Nanoeng. 8, 1–22.
Downs, A.M., Gerson, J., Ploense, K.L., Plaxco, K.W., Dauphin-Ducharme, P., 2020. Anal. Chem. 92, 14063–14068.
Elbrecht, D.H., Hickman, C.J.L., J, J., 2016. J. Rare Dis. Res. Treat. 1.
Eltzov, E., Marks, R.S., 2011. Anal. Bioanal. Chem. 400, 895–913.
Esch, E.W., Bahinski, A., Huh, D., 2015. Nat. Rev. Drug Discov. 14, 248–260.
Falanga, A.P., Pitingolo, G., Celentano, M., Cosentino, A., Melone, P., Vecchione, R., Guarnieri, D., Netti, P.A., 2017. Biotechnol. Bioeng. 114, 1087–1095.
Farooqi, H.M.U., Khalid, M.A.U., Kim, K.H., Lee, S.R., Choi, K.H., 2020. J. Micromech. Microeng. 30, 115013.
Figueiredo, L., Le Visage, C., Weiss, P., Yang, J., 2020. Polymers 12, 1260.
Fisher, C.R., Medie, F.M., Luu, R.J., Quezada, L.L., Gaibler, R.B., Mulhern, T.J., Rubio, L. D., Marr, E.E., Gabriel, E.P., Borenstein, J.T., Gard, A.L., 2022. bioRxiv. https://doi.org/10.1101/2022.06.07.495101.
Frese, L., Darwiche, S.E., von Rechenberg, B., Hoerstrup, S.P., Giovanoli, P., Calcagni, M., 2021. Cytotherapy 23, 536–547.
Freshney, R.I., 2010a. Laboratory design, layout, and equipment. In: Culture of Animal Cells: A Manual of Basic Technique and Specialized Applications. John Wiley & Sons, Ltd., Hoboken, New Jersey, USA, pp. 25–36.
Freshney, R.I., 2010b. Defined media and supplements. In: Culture of Animal Cells: A Manual of Basic Technique and Specialized Applications. John Wiley & Sons, Ltd., Hoboken, New Jersey, USA, pp. 99–114.
Fuchs, S., Johansson, S., Tjell, A.Ø., Werr, G., Mayr, T., Tenje, M., 2021. ACS Biomater. Sci. Eng. 7, 2926–2948.

Galan, E.A., Zhao, H., Wang, X., Dai, Q., Huck, W.T.S., Ma, S., 2020. Matter. 3, 1893–1922.
Gard, A.L., Luu, R.J., Miller, C.R., Maloney, R., Cain, B.P., Marr, E.E., Burns, D.M., Gaibler, R., Mulhern, T.J., Wong, C.A., Alladina, J., Coppeta, J.R., Liu, P., Wang, J.P., Azizgolshani, H., Fezzie, R.F., Balestrini, J.L., Isenberg, B.C., Medoff, B.D., Finberg, R.W., Borenstein, J.T., 2021. Sci. Rep. 11, 14961.
Go, D.B., Atashbar, M.Z., Ramshani, Z., Chang, H.-C., 2017. Anal. Methods 9, 4112–4134.
Goode, J.A., Rushworth, J.V.H., Millner, P.A., 2015. Langmuir 31, 6267–6276.
Griendling, K.K., Touyz, R.M., Zweier, J.L., Dikalov, S., Chilian, W., Chen, Y.-R., Harrison, D.G., Bhatnagar, A., 2016. Circ. Res. 119, e39–e75.
Ham, R.G., Puck, T.T., 1962. Exp. Biol. Med. 111, 67–71.
Han, S.J., Kwon, S., Kim, K.S., 2021. Cancer Cell Int. 21, 152.
Hassan, M.H., Vyas, C., Grieve, B., Bartolo, P., 2021. Sensors 21, 4672.
van der Helm, M.W., Odijk, M., Frimat, J.-P., van der Meer, A.D., Eijkel, J.C.T., van den Berg, A., Segerink, L.I., 2016. Biosens. Bioelectron. 85, 924–929.
van der Helm, M.W., Odijk, M., Frimat, J.-P., van der Meer, A.D., Eijkel, J.C.T., van den Berg, A., Segerink, L.I., 2017. JoVE J. Vis. Exp., e56334
Henry, O.Y.F., Villenave, R., Cronce, M.J., Leineweber, W.D., Benz, M.A., Ingber, D.E., 2017. Lab Chip 17, 2264–2271.
Herland, A., Meer van der, A.D., FitzGerald, E.A., Park, T.-E., Sleeboom, J.J.F., Ingber, D. E., 2016. PLoS One 11, e0150360.
Hernández-Ramírez, D., Mendoza-Huizar, L.H., Galán-Vidal, C.A., Aguilar-Lira, G.Y., Álvarez-Romero, G.A., 2021. J. Electrochem. Soc. 168, 057522.
Hodgkin, A.L., Huxley, A.F., 1952. J. Physiol. 117, 500–544.
Hu, J., Stein, A., Bühlmann, P., 2016. TrAC, Trends Anal. Chem. 76, 102–114.
Huh, D., Matthews, B.D., Mammoto, A., Montoya-Zavala, M., Hsin, H.Y., Ingber, D.E., 2010. Science 328, 1662–1668.
Hwang, D.-W., Lee, S., Seo, M., Chung, T.D., 2018. Anal. Chim. Acta 1033, 1–34.
Ingber, D.E., 2022. Nat. Rev. Genet. 23, 467–491.
Isozaki, A., Harmon, J., Zhou, Y., Li, S., Nakagawa, Y., Hayashi, M., Mikami, H., Lei, C., Goda, K., 2020. Lab Chip 20, 3074–3090.
Jalili-Firoozinezhad, S., Gazzaniga, F.S., Calamari, E.L., Camacho, D.M., Fadel, C.W., Bein, A., Swenor, B., Nestor, B., Cronce, M.J., Tovaglieri, A., Levy, O., Gregory, K.E., Breault, D.T., Cabral, J.M.S., Kasper, D.L., Novak, R., Ingber, D.E., 2019. Nat. Biomed. Eng. 3, 520–531.
Jang, K.-J., Mehr, A.P., Hamilton, G.A., McPartlin, L.A., Chung, S., Suh, K.-Y., Ingber, D. E., 2013. Integr. Biol. 5, 1119–1129.
Janshoff, A., Kunze, A., Michaelis, S., Heitmann, V., Reiss, B., Wegener, J., 2010. J. Adhes. Sci. Technol. 24, 2079–2104.
Jeon, M.S., Choi, Y.Y., Mo, S.J., Ha, J.H., Lee, Y.S., Lee, H.U., Park, S.D., Shim, J.-J., Lee, J.-L., Chung, B.G., 2022. Nano Converg. 9, 8.
Jiang, C., Wang, G., Hein, R., Liu, N., Luo, X., Davis, J.J., 2020. Chem. Rev. 120, 3852–3889.
Karimzadeh, A., Hasanzadeh, M., Shadjou, N., de la Guardia, M., 2018. TrAC, Trends Anal. Chem. 107, 1–20.
Kattipparambil Rajan, D., Verho, J., Kreutzer, J., Välimäki, H., Ihalainen, H., Lekkala, J., Patrikoski, M., Miettinen, S., 2017. Monitoring pH, temperature and humidity in long-term stem cell culture in CO2 incubator. In: 2017 IEEE International Symposium on Medical Measurements and Applications (MeMeA). Presented at the 2017 IEEE International Symposium on Medical Measurements and Applications. MeMeA), pp. 470–474.
Kavand, H., Nasiri, R., Herland, A., 2022. Adv. Mater. 34, 2107876.
Kemas, A.M., Youhanna, S., Zandi Shafagh, R., Lauschke, V.M., 2021. Faseb. J. 35, e21305.
Khalid, M.A.U., Kim, Y.S., Ali, M., Lee, B.G., Cho, Y.-J., Choi, K.H., 2020. Biochem. Eng. J. 155, 107469.
Kilic, T., Navaee, F., Stradolini, F., Renaud, P., Carrara, S., 2018. Microphysiol. Syst. 2, 1–32.
Kim, H.J., Ingber, D.E., 2013. Integr. Biol. 5, 1130–1140.
Kim, S., Lee, H., Chung, M., Jeon, N.L., 2013. Lab Chip 13, 1489–1500.
Kim, S.B., Koo, K., Bae, H., Dokmeci, M.R., Hamilton, G.A., Bahinski, A., Kim, S.M., Ingber, D.E., Khademhosseini, A., 2012. Lab Chip 12, 3976–3982.
Kléber, A.G., Rudy, Y., 2004. Physiol. Rev. 84, 431–488.
Kokkinos, C., Economou, A., Prodromidis, M.I., 2016. TrAC, Trends Anal. Chem. 79, 88–105.
Kujala, V.J., Pasqualini, F.S., Goss, J.A., Nawroth, J.C., Parker, K.K., 2016. J. Mater. Chem. B 4, 3534–3543.
Langer, J., Jimenez de Aberasturi, D., Aizpurua, J., Alvarez-Puebla, R.A., Auguié, B., Baumberg, J.J., Bazan, G.C., Bell, S.E.J., Boisen, A., Brolo, A.G., Choo, J., Cialla-May, D., Deckert, V., Fabris, L., Faulds, K., García de Abajo, F.J., Goodacre, R., Graham, D., Haes, A.J., Haynes, C.L., Huck, C., Itoh, T., Käll, M., Kneipp, J., Kotov, N.A., Kuang, H., Le Ru, E.C., Lee, H.K., Li, J.-F., Ling, X.Y., Maier, S.A., Mayerhöfer, T., Moskovits, M., Murakoshi, K., Nam, J.-M., Nie, S., Ozaki, Y., Pastoriza-Santos, I., Perez-Juste, J., Popp, J., Pucci, A., Reich, S., Ren, B., Schatz, G. C., Shegai, T., Schlücker, S., Tay, L.-L., Thomas, K.G., Tian, Z.-Q., Van Duyne, R.P., Vo-Dinh, T., Wang, Y., Willets, K.A., Xu, C., Xu, H., Xu, Y., Yamamoto, Y.S., Zhao, B., Liz-Marzán, L.M., 2020. ACS Nano 14, 28–117.
Lee, C.S., Leong, K.W., 2020. Curr. Opin. Biotechnol., Tissue, Cell and Pathway Engineering 66, 78–87.
Lee, J., Mehrotra, S., Zare-Eelanjegh, E., Rodrigues, R.O., Akbarinejad, A., Ge, D., Amato, L., Kiaee, K., Fang, Y., Rosenkranz, A., Keung, W., Mandal, B.B., Li, R.A., Zhang, T., Lee, H., Dokmeci, M.R., Zhang, Y.S., Khademhosseini, A., Shin, S.R., 2021. Small 17, 2004258.
Leung, C.M., de Haan, P., Ronaldson-Bouchard, K., Kim, G.-A., Ko, J., Rho, H.S., Chen, Z., Habibovic, P., Jeon, N.L., Takayama, S., Shuler, M.L., Vunjak-Novakovic, G., Frey, O., Verpoorte, E., Toh, Y.-C., 2022. Nat. Rev. Methods Primer 2, 1–29.
Li, J., Chen, J., Bai, H., Wang, H., Hao, S., Ding, Y., Peng, B., Zhang, J., Li, L., Huang, W., 2022. Research 2022.
Li Sella, C., Lemaître, F., Guille-Collignon, M., Amatore, C., Thouin, L., 2018. Anal. Chem. 90, 9386–9394.
Li, X., Soler, M., Özdemir, C.I., Belushkin, A., Yesilköy, F., Altug, H., 2017. Lab Chip 17, 2208–2217.
Li, X., Tian, T., 2018. Anal. Methods 10, 3122–3130.
Liao, Z., Zhang, Y., Li, Y., Miao, Y., Gao, S., Lin, F., Deng, Y., Geng, L., 2019. Biosens. Bioelectron. 126, 697–706.
Lin, A., Sved Skottvoll, F., Rayner, S., Pedersen-Bjergaard, S., Sullivan, G., Krauss, S., Ray Wilson, S., Harrison, S., 2020. Electrophoresis 41, 56–64.
Lind, J.U., Yadid, M., Perkins, I., O'Connor, B.B., Eweje, F., Chantre, C.O., Hemphill, M. A., Yuan, H., Campbell, P.H., Vlassak, J.J., Parker, K.K., 2017. Lab Chip 17, 3692–3703.
Liu, L., Bi, M., Wang, Y., Liu, J., Jiang, X., Xu, Z., Zhang, X., 2021. Nanoscale 13, 19352–19366.
Liu, Y., Liu, Y., Matharu, Z., Rahimian, A., Revzin, A., 2015. Biosens. Bioelectron. 64, 43–50.
Liu, Y., Zhang, X., 2021. Micromachines 12, 826.
Low, L.A., Mummery, C., Berridge, B.R., Austin, C.P., Tagle, D.A., 2021. Nat. Rev. Drug Discov. 20, 345–361.
Ma, C., Fan, R., Ahmad, H., Shi, Q., Comin-Anduix, B., Chodon, T., Koya, R.C., Liu, C.-C., Kwong, G.A., Radu, C.G., Ribas, A., Heath, J.R., 2011. Nat. Med. 17, 738–743.
MacDonald, P.E., Rorsman, P., 2006. PLoS Biol. 4, e49.
Maduraiveeran, G., Sasidharan, M., Ganesan, V., 2018. Biosens. Bioelectron. 103, 113–129.
Maganzini, N., Thompson, I., Wilson, B., Soh, H.T., 2022. Pre-equilibrium Biosensors: A New Approach towards Rapid and Continuous Molecular Measurements (Preprint). Bioengineering.
Maioli, V., Chennell, G., Sparks, H., Lana, T., Kumar, S., Carling, D., Sardini, A., Dunsby, C., 2016. Sci. Rep. 6, 37777.
Maoz, B.M., Herland, A., Henry, O.Y.F., Leineweber, W.D., Yadid, M., Doyle, J., Mannix, R., Kujala, V.J., FitzGerald, E.A., Parker, K.K., Ingber, D.E., 2017. Lab Chip 17, 2294–2302.
Martín-Palma, R.J., 2021. Absorbance biosensors. In: Field Guide to Optical Biosensing. SPIE, Bellingham, Washington, USA.
Marx, K.A., Zhou, T., Montrone, A., Schulze, H., Braunhut, S.J., 2001. Biosens. Bioelectron. 16, 773–782.
Matharu, Z., Patel, D., Gao, Y., Haque, A., Zhou, Q., Revzin, A., 2014. Anal. Chem. 86, 8865–8872.
Matsumoto, S., Leclerc, E., Maekawa, T., Kinoshita, H., Shinohara, M., Komori, K., Sakai, Y., Fujii, T., 2018. Sensor. Actuator. B Chem. 273, 1062–1069.
Mencattini, A., Di Giuseppe, D., Comes, M.C., Casti, P., Corsi, F., Bertani, F.R., Ghibelli, L., Businaro, L., Di Natale, C., Parrini, M.C., Martinelli, E., 2020. Sci. Rep. 10, 7653.
Mermoud, Y., Felder, M., Stucki, A.O., Guenat, O.T., 2018. Sensor. Actuator. B Chem. 255, 3647–3653.
Misun, P.M., Rothe, J., Schmid, Y.R.F., Hierlemann, A., Frey, O., 2016. Microsyst. Nanoeng. 2, 16022.
Miyazaki, T., Hirai, Y., Kamei, K., Tsuchiya, T., Tabata, O., 2021. Electron. Commun. Jpn. 104, e12296.
Moshksayan, K., Kashaninejad, N., Warkiani, M.E., Lock, J.G., Moghadas, H., Firoozabadi, B., Saidi, M.S., Nguyen, N.-T., 2018. Sensor. Actuator. B Chem. 263, 151–176.
Mousavi Shaegh, S.A., De Ferrari, F., Zhang, Y.S., Nabavinia, M., Binth Mohammad, N., Ryan, J., Pourmand, A., Laukaitis, E., Banan Sadeghian, R., Nadhman, A., Shin, S.R., Nezhad, A.S., Khademhosseini, A., Dokmeci, M.R., 2016. Biomicrofluidics 10, 044111.
Moya, A., Ortega-Ribera, M., Guimerà, X., Sowade, E., Zea, M., Illa, X., Ramon, E., Villa, R., Gracia-Sancho, J., Gabriel, G., 2018. Lab Chip 18, 2023–2035.
Nasr, B., Chatterton, R., Yong, J.H.M., Jamshidi, P., D'Abaco, G.M., Bjorksten, A.R., Kavehei, O., Chana, G., Dottori, M., Skafidas, E., 2018. Biosensors 8, 14.
Nguyen, H.H., Lee, S.H., Lee, U.J., Fermin, C.D., Kim, M., 2019. Materials 12, 121.
Novak, R., Ingram, M., Marquez, S., Das, D., Delahanty, A., Herland, A., Maoz, B.M., Jeanty, S.S.F., Somayaji, M.R., Burt, M., Calamari, E., Chalkiadaki, A., Cho, A., Choe, Y., Chou, D.B., Cronce, M., Dauth, S., Divic, T., Fernandez-Alcon, J., Ferrante, T., Ferrier, J., FitzGerald, E.A., Fleming, R., Jalili-Firoozinezhad, S., Grevesse, T., Goss, J.A., Hamkins-Indik, T., Henry, O., Hinojosa, C., Huffstater, T., Jang, K.-J., Kujala, V., Leng, L., Mannix, R., Milton, Y., Nawroth, J., Nestor, B.A., Ng, C.F., O'Connor, B., Park, T.-E., Sanchez, H., Sliz, J., Sontheimer-Phelps, A., Swenor, B., Thompson II, G., Touloumes, G.J., Tranchemontagne, Z., Wen, N., Yadid, M., Bahinski, A., Hamilton, G.A., Levner, D., Levy, O., Przekwas, A., Prantil-Baun, R., Parker, K.K., Ingber, D.E., 2020. Nat. Biomed. Eng. 4, 407–420.
Obregón, R., Ahadian, S., Ramón-Azcón, J., Chen, L., Fujita, T., Shiku, H., Chen, M., Matsue, T., 2013. Biosens. Bioelectron. 50, 194–201.
Okkelman, I.A., Neto, N., Papkovsky, D.B., Monaghan, M.G., Dmitriev, R.I., 2020. Redox Biol. 30, 101420.
Ortega, M.A., Fernández-Garibay, X., Castaño, A.G., de Chiara, F., Hernández-Albors, A., Balaguer-Trias, J., Ramón-Azcón, J., 2019. Lab Chip 19, 2568–2580.
Ortega, M.A., Rodríguez-Comas, J., Yavas, O., Velasco-Mallorquí, F., Balaguer-Trias, J., Parra, V., Novials, A., Servitja, J.M., Quidant, R., Ramón-Azcón, J., 2021. Biosensors 11, 138.
Osaki, T., Uzel, S.G.M., Kamm, R.D., 2018. Sci. Adv. 4, eaat5847.

Paramasivam, K., Shen, Y., Yuan, J., Waheed, I., Mao, C., Zhou, X., 2022. Biosensors 12, 30.
Park, T.-E., Mustafaoglu, N., Herland, A., Hasselkus, R., Mannix, R., FitzGerald, E.A., Prantil-Baun, R., Watters, A., Henry, O., Benz, M., Sanchez, H., McCrea, H.J., Goumnerova, L.C., Song, H.W., Palecek, S.P., Shusta, E., Ingber, D.E., 2019. Nat. Commun. 10, 2621.
Pires, N.M.M., Dong, T., Hanke, U., Hoivik, N., 2014. Sensors 14, 15458–15479.
Pohanka, M., 2017. Int. J. Electrochem. Sci. 8082–8094.
da Ponte, R.M., Gaio, N., van Zeijl, H., Vollebregt, S., Dijkstra, P., Dekker, R., Serdijn, W. A., Giagka, V., 2021. Sens. Actuators Phys. 317, 112439.
Quinn, P.J., 1988. Symp. Soc. Exp. Biol. 42, 237–258.
Rafique, B., Iqbal, M., Mehmood, T., Shaheen, M.A., 2019. Sens. Rev. 39, 34–50.
Rennert, K., Steinborn, S., Gröger, M., Ungerböck, B., Jank, A.-M., Ehgartner, J., Nietzsche, S., Dinger, J., Kiehntopf, M., Funke, H., Peters, F.T., Lupp, A., Gärtner, C., Mayr, T., Bauer, M., Huber, O., Mosig, A.S., 2015. Biomaterials 71, 119–131.
Riahi, R., Shaegh, S.A.M., Ghaderi, M., Zhang, Y.S., Shin, S.R., Aleman, J., Massa, S., Kim, D., Dokmeci, M.R., Khademhosseini, A., 2016. Sci. Rep. 6, 24598.
Ro, J., Kim, J., Cho, Y.-K., 2022. Analyst 147, 2023–2034.
Roda, A., Mirasoli, M., Michelini, E., Di Fusco, M., Zangheri, M., Cevenini, L., Roda, B., Simoni, P., 2016. Biosens. Bioelectron. 76, 164–179.
Rothbauer, M., Höll, G., Eilenberger, C., Kratz, S.R.A., Farooq, B., Schuller, P., Calvo, I. O., Byrne, R.A., Meyer, B., Niederreiter, B., Küpcü, S., Sevelda, F., Holinka, J., Hayden, O., Tedde, S.F., Kiener, H.P., Ertl, P., 2020. Lab Chip 20, 1461–1471.
Sabaté del Río, J., Henry, O.Y.F., Jolly, P., Ingber, D.E., 2019. Nat. Nanotechnol. 14, 1143–1149.
Sabaté del Río, J., Woo, H.-K., Park, J., Ha, H.K., Kim, J.-R., Cho, Y.-K., 2022. Adv. Mater. 34, 2200981.
Sakamiya, M., Fang, Y., Mo, X., Shen, J., Zhang, T., 2020. Med. Eng. Phys. 75, 36–44.
Santos, A.L., Sinha, S., Lindner, A.B., 2018. Oxid. Med. Cell. Longev. 2018, e1941285.
Schieber, M., Chandel, N.S., 2014. Curr. Biol. 24, R453–R462.
Schmid, Y.R.F., Bürgel, S.C., Misun, P.M., Hierlemann, A., Frey, O., 2016. ACS Sens. 1, 1028–1035.
Schmidt-Speicher, L.M., Länge, K., 2021. Curr. Opin. Electrochem. 29, 100755.
Schneider, G., 2018. Nat. Rev. Drug Discov. 17, 97–113.
Schneider, O., Moruzzi, A., Fuchs, S., Grobel, A., Schulze, H.S., Mayr, T., Loskill, P., 2022. Mater. Today Bio. 15, 100280.
Serebrennikova, K.V., Berlina, A.N., Sotnikov, D.V., Zherdev, A.V., Dzantiev, B.B., 2021. Biosensors 11, 512.
Shakhih, M.F.M., Rosslan, A.S., Noor, A.M., Ramanathan, S., Lazim, A.M., Wahab, A.A., 2021. J. Electrochem. Soc. 168, 067502.
Shamkhalichenar, H., Choi, J.-W., 2020. J. Electrochem. Soc. 167, 037531.
Sharma, R., Roychoudhury, S., Singh, N., Sarda, Y., 2017. Methods to measure reactive oxygen species (ROS) and total antioxidant capacity (TAC) in the reproductive system. In: Agarwal, A., Sharma, R., Gupta, S., Harlev, A., Ahmad, G., du Plessis, S.S., Esteves, S.C., Wang, S.M., Durairajanayagam, D. (Eds.), Oxidative Stress in Human Reproduction. Springer International Publishing, Cham, Switzerland, pp. 17–46.
Shaughnessey, E.M., Kann, S.H., Azizgolshani, H., Black, L.D., Charest, J.L., Vedula, E.M., 2022. Sci. Rep. 12, 13182.
Shi, H., Nie, K., Dong, B., Long, M., Xu, H., Liu, Z., 2019. Chem. Eng. J. 361, 635–650.
Shin, S.R., Zhang, Y.S., Kim, D.-J., Manbohi, A., Avci, H., Silvestri, A., Aleman, J., Hu, N., Kilic, T., Keung, W., Righi, M., Assawes, P., Alhadrami, H.A., Li, R.A., Dokmeci, M.R., Khademhosseini, A., 2016. Anal. Chem. 88, 10019–10027.
Sidorov, V.Y., Samson, P.C., Sidorova, T.N., Davidson, J.M., Lim, C.C., Wikswo, J.P., 2017. Acta Biomater. 48, 68–78.
Sinenko, S.A., Starkova, T.Yu, Kuzmin, A.A., Tomilin, A.N., 2021. Front. Cell Dev. Biol. 9, 714370.
Singh, A., Sharma, A., Ahmed, A., Sundramoorthy, A.K., Furukawa, H., Arya, S., Khosla, A., 2021. Biosensors 11, 336.
Škrlec, K., Štrukelj, B., Berlec, A., 2015. Trends Biotechnol. 33, 408–418.
Son, K.J., Gheibi, P., Stybayeva, G., Rahimian, A., Revzin, A., 2017. Microsyst. Nanoeng. 3, 17025.
Soomro, A.M., Jabbar, F., Ali, M., Lee, J.-W., Mun, S.W., Choi, K.H., 2019. J. Mater. Sci. Mater. Electron. 30, 9455–9465.
Spira, M.E., Hai, A., 2013. Nat. Nanotechnol. 8, 83–94.
Suzuki, H., Hirakawa, T., Watanabe, I., Kikuchi, Y., 2001. Anal. Chim. Acta 431, 249–259.
Tak For Yu, Z., Guan, H., Ki Cheung, M., McHugh, W.M., Cornell, T.T., Shanley, T.P., Kurabayashi, K., Fu, J., 2015. Sci. Rep. 5, 11339.
Takehara, H., Kazutaka, O., Haruta, M., Noda, T., Sasagawa, K., Tokuda, T., Ohta, J., 2017. AIP Adv. 7, 095213.
Tan, X.H.M., Ngyuen, A.V., Rowat, A.C., Chiou, P.-Y., 2018. Large area precision cell traction force measurements using gold disk mounted micro-pillars. In: 2018 IEEE 12th International Conference on Nano/Molecular Medicine and Engineering (NANOMED). Presented at the 2018 IEEE 12th International Conference on Nano/Molecular Medicine and Engineering. NANOMED), pp. 100–103.
Tanumihardja, E., Slaats, R.H., van der Meer, A.D., Passier, R., Olthuis, W., van den Berg, A., 2021. ACS Sens. 6, 267–274.
Tipparaju, V.V., Mora, S.J., Yu, J., Tsow, F., Xian, X., 2021. IEEE Sensor. J. 21, 17327–17334.
Ugolini, G.S., Occhetta, P., Saccani, A., Re, F., Krol, S., Rasponi, M., Redaelli, A., 2018. J. Micromech. Microeng. 28, 044001.
Uhlén, M., Karlsson, M.J., Hober, A., Svensson, A.-S., Scheffel, J., Kotol, D., Zhong, W., Tebani, A., Strandberg, L., Edfors, F., Sjöstedt, E., Mulder, J., Mardinoglu, A., Berling, A., Ekblad, S., Dannemeyer, M., Kanje, S., Rockberg, J., Lundqvist, M., Malm, M., Volk, A.-L., Nilsson, P., Månberg, A., Dodig-Crnkovic, T., Pin, E., Zwahlen, M., Oksvold, P., von Feilitzen, K., Häussler, R.S., Hong, M.-G., Lindskog, C., Ponten, F., Katona, B., Vuu, J., Lindström, E., Nielsen, J., Robinson, J., Ayoglu, B., Mahdessian, D., Sullivan, D., Thul, P., Danielsson, F., Stadler, C., Lundberg, E., Bergström, G., Gummesson, A., Voldborg, B.G., Tegel, H., Hober, S., Forsström, B., Schwenk, J.M., Fagerberg, L., Sivertsson, Å., 2019. Sci. Signal. 12, eaaz0274.
Vatine, G.D., Barrile, R., Workman, M.J., Sances, S., Barriga, B.K., Rahnama, M., Barthakur, S., Kasendra, M., Lucchesi, C., Kerns, J., Wen, N., Spivia, W.R., Chen, Z., Van Eyk, J., Svendsen, C.N., 2019. Cell Stem Cell 24, 995–1005.e6.
Wang, Y.I., Abaci, H.E., Shuler, M.L., 2017. Biotechnol. Bioeng. 114, 184–194.
Wei, X., Gu, C., Li, H., Pan, Y., Zhang, B., Zhuang, L., Wan, H., Hu, N., Wang, P., 2019. Sensor. Actuator. B Chem. 283, 881–889.
Weltin, A., Hammer, S., Noor, F., Kaminski, Y., Kieninger, J., Urban, G.A., 2017. Biosens. Bioelectron. 87, 941–948.
Weltin, A., Slotwinski, K., Kieninger, J., Moser, I., Jobst, G., Wego, M., Ehret, R., Urban, G.A., 2014. Lab Chip 14, 138–146.
Wikswo, J.P., Block III, F.E., Cliffel, D.E., Goodwin, C.R., Marasco, C.C., Markov, D.A., McLean, D.L., McLean, J.A., McKenzie, J.R., Reiserer, R.S., Samson, P.C., Schaffer, D. K., Seale, K.T., Sherrod, S.D., 2013. IEEE Trans. Biomed. Eng. 60, 682–690.
Wishart, D.S., Guo, A., Oler, E., Wang, F., Anjum, A., Peters, H., Dizon, R., Sayeeda, Z., Tian, S., Lee, B.L., Berjanskii, M., Mah, R., Yamamoto, M., Jovel, J., Torres-Calzada, C., Hiebert-Giesbrecht, M., Lui, V.W., Varshavi, Dorna, Varshavi, Dorsa, Allen, D., Arndt, D., Khetarpal, N., Sivakumaran, A., Harford, K., Sanford, S., Yee, K., Cao, X., Budinski, Z., Liigand, J., Zhang, L., Zheng, J., Mandal, R., Karu, N., Dambrova, M., Schiöth, H.B., Greiner, R., Gautam, V., 2022. Nucleic Acids Res. 50, D622–D631.
Wong, C.H., Siah, K.W., Lo, A.W., 2019. Biostatistics 20, 273–286.
Wu, G., Wu, J., Li, Z., Shi, S., Wu, D., Wang, X., Xu, H., Liu, H., Huang, Y., Wang, R., Shen, J., Dong, Z., Wang, S., 2022. Bio-des. Man 5, 437–450.
Yang, H., Peng, Y., Xu, M., Xu, S., Zhou, Y., 2021. Crit. Rev. Anal. Chem. 1–16.
Young, A.T., Rivera, K.R., Erb, P.D., Daniele, M.A., 2019. ACS Sens. 4, 1454–1464.
Zare Harofte, S., Soltani, M., Siavashy, S., Raahemifar, K., 2022. Small 18, 2203169.
Zbinden, A., Marzi, J., Schlünder, K., Probst, C., Urbanczyk, M., Black, S., Brauchle, E.M., Layland, S.L., Kraushaar, U., Duffy, G., Schenke-Layland, K., Loskill, P., 2020. Matrix Biol., Matrix Biomechanics 85–86, 205–220.
Zeitouni, N.E., Chotikatum, S., von Köckritz-Blickwede, M., Naim, H.Y., 2016. Mol. Cell. Pediatr. 3, 14.
Zervantonakis, I.K., Arvanitis, C.D., 2016. Small 12, 2616–2626.
Zhang, X., Jang, S., 2018. Int. J. Biosens. Bioelectron. 4, 260–261.
Zhang, Y.S., Aleman, J., Shin, S.R., Kilic, T., Kim, D., Mousavi Shaegh, S.A., Massa, S., Riahi, R., Chae, S., Hu, N., Avci, H., Zhang, W., Silvestri, A., Sanati Nezhad, A., Manbohi, A., De Ferrari, F., Polini, A., Calzone, G., Shaikh, N., Alerasool, P., Budina, E., Kang, J., Bhise, N., Ribas, J., Pourmand, A., Skardal, A., Shupe, T., Bishop, C.E., Dokmeci, M.R., Atala, A., Khademhosseini, A., 2017. Proc. Natl. Acad. Sci. USA 114, E2293–E2302.
Zhang, Y.S., Ribas, J., Nadhman, A., Aleman, J., Selimović, Š., Lesher-Perez, S.C., Wang, T., Manoharan, V., Shin, S.-R., Damilano, A., Annabi, N., Dokmeci, M.R., Takayama, S., Khademhosseini, A., 2015. Lab Chip 15, 3661–3669.
Zhao, X., Gao, W., Yin, J., Fan, W., Wang, Z., Hu, K., Mai, Y., Luan, A., Xu, B., Jin, Q., 2021. Talanta 226, 122101.
Zhao, Y., Rafatian, N., Wang, E.Y., Feric, N.T., Lai, B.F.L., Knee-Walden, E.J., Backx, P.H., Radisic, M., 2020. Matrix Biol. 85–86, 189–204.
Zhao, Y., Yavari, K., Liu, J., 2022. TrAC, Trends Anal. Chem. 146, 116480.
Zhou, Q., Kwa, T., Gao, Y., Liu, Y., Rahimian, A., Revzin, A., 2014. Lab Chip 14, 276–279.
Zhou, Q., Patel, D., Kwa, T., Haque, A., Matharu, Z., Stybayeva, G., Gao, Y., Diehl, A.M., Revzin, A., 2015. Lab Chip 15, 4467–4478.
Zhou, Y., Danbolt, N.C., 2014. J. Neural. Transm. 121, 799–817.
Zhu, J., He, J., Verano, M., Brimmo, A.T., Glia, A., Qasaimeh, M.A., Chen, P., Aleman, J. O., Chen, W., 2018. Lab Chip 18, 3550–3560.
Zuchowska, A., Marciniak, K., Bazylinska, U., Jastrzebska, E., Wilk, K.A., Brzozka, Z., 2018. Sensor. Actuator. B Chem. 275, 69–77.